EYELESS LEADS THE WAY: ENGINEERING A NEURONAL CIRCUIT FOR NAVIGATION IN *DROSOPHILA*

by

LUIS F. SULLIVAN

A DISSERTATION

Presented to the Department of Biology
and the Graduate School of the University of Oregon
in partial fulfillment of the requirements
for the degree of
Doctor of Philosophy

June 2019

DISSERTATION APPROVAL PAGE

Student: Luis F. Sullivan

Title: Eyeless Leads the Way: Engineering a Neuronal Circuit for Navigation in Drosophila

This dissertation has been accepted and approved in partial fulfillment of the requirements for the Doctor of Philosophy degree in the Biology by:

Cris Niell	Chairperson
Chris Doe	Advisor
Tory Herman	Core Member
Bruce Bowerman	Core Member
Mike Wehr	Institutional Representative

and

Janet Woodruff-Borden	Vice Provost and Dean of the Graduate School

Original approval signatures are on file with the University of Oregon Graduate School.

Degree awarded June 2019

© 2019 Luis F. Sullivan

DISSERTATION ABSTRACT

Luis F. Sullivan

Doctor of Philosophy

Department of Biology

June 2019

Title: Eyeless Leads the Way: Engineering a Neuronal Circuit for Navigation in *Drosophila*

The insect central complex (CX) is a conserved brain region containing 60+ neuronal subtypes, several of which contribute to navigation. It is not known how CX neuronal diversity is generated or how developmental origin of subtypes relates to function. We mapped the developmental origin of four key CX subtypes and found that neurons with similar origin have similar axon/dendrite targeting. Moreover, we found that the temporal transcription factor (TTF) Eyeless/Pax6 regulates the development of two recurrently-connected CX subtypes: Eyeless loss simultaneously produces ectopic P-EN neurons with normal axon/dendrite projections, and reduces the number of E-PG neurons. Furthermore, transient loss of Eyeless during development impairs adult flies' capacity to perform celestial navigation. We conclude that neurons with similar developmental origin have similar connectivity, that Eyeless maintains equal E-PG and P-EN neuron number, and that Eyeless is required for the development of circuits that control adult navigation.

This dissertation includes previously published and/or co-authored material. Reproduced with permission from: Sullivan, L. F., Warren, T. L., & Doe, C. Q. (2019) Temporal identity establishes columnar neuron morphology, connectivity, and function in a Drosophila navigation circuit. *eLife*

CURRICULUM VITAE

NAME OF AUTHOR: Luis F. Sullivan

GRADUATE AND UNDERGRADUATE SCHOOLS ATTENDED:

University of Oregon, Eugene
George Mason University, Fairfax

DEGREES AWARDED:

Bachelor of Science, Neuroscience, 2013 George Mason University

AREAS OF SPECIAL INTEREST:

Drosophila neurobiology and genetics

PROFESSIONAL EXPERIENCE:

Postbaccalaureate Research Fellow, National Institutes of Health, 2013

GRANTS, AWARDS, AND HONORS:

Developmental Biology Training Grant, University of Oregon, 2015-2018

PUBLICATIONS:

Sullivan, L. F., Warren, T. L., & Doe, C. Q. (2019) Temporal identity establishes columnar neuron morphology, connectivity, and function in a Drosophila navigation circuit. *eLife*

Sullivan, L. F. (2019). Rewiring the Drosophila brain with genetic manipulations in neural lineages. *Frontiers in Molecular Neuroscience*

ACKNOWLEDGMENTS

I would like to thank my mentor, Chris Q. Doe, for giving me the freedom to build this project from the ground up. His guidance was invaluable during the entire process within the lab. I would also like to thank my friend, Brandt Stuart, for his tireless support for me outside the lab.

TABLE OF CONTENTS

LIST OF FIGURES

LIST OF TABLES

Table Page

CHAPTER I: INTRODUCTION

This chapter includes previously published and/or co-authored material. Reproduced with permission in Chapter II from: Sullivan, L. F., Warren, T. L., & Doe, C. Q. (2019) Temporal identity establishes columnar neuron morphology, connectivity, and function in a Drosophila navigation circuit. *eLife*
Reproduced in Chapter I from: Sullivan, L. F. (2019). Rewiring the Drosophila brain with genetic manipulations in neural lineages. *Frontiers in Molecular Neuroscience*

Brains are made of millions of neurons, which communicate with one another to drive all forms of cognition and behavior. Neurons have diverse functions in the brain, ranging from post-sensory processing to subsequent computations for behavior (Gold and Shadlen 2001; Shadlen et al. 1996). To function properly, neurons must assemble into complex, anatomically stereotyped circuits. Assembling such anatomical circuits, or maps, requires precise dendritic patterning, axonal targeting, and synapse partnering. These components of circuit development require a range of molecular and genetic mechanisms, from expression of cell-surface molecules for local cell-cell interactions, to transcription factors (Enriquez et al. 2015; Williams et al. 2010; Dickson 2003; Tada and Sheng 2006). Neuronal subtypes can express entirely different cell-surface molecules and transcription factors, which likely accounts for much of their anatomical and functional diversity in the adult brain. One possibility is that the mechanisms that establish molecular diversity in the brain as neurons are generated are independent from those that establish connectivity.

From work in *Drosophila*, however, a picture emerges where molecular mechanisms during neurogenesis can rewire precise circuit anatomy when genetically manipulated, which implicates genes generating neuronal identity as direct regulators of circuit assembly (Sen et al. 2014; Kao et al. 2012; Pinto-Teixeira et al. 2018; Sullivan et al. 2019).

Drosophila neural progenitors, called neuroblasts, express specific factors across both spatial and temporal axes. Initially, as ventral nerve cord (VNC) neuroblasts delaminate from the neuroepithelium, they express *spatial cues* based on where they delaminate (Skeath and Thor 2003; Truman and Bate 1988) (Figure 1A). From here, they express *temporal cues* as they age and generate neural progeny (Doe 2017) (Figure 1B). Finally, as ganglion-mother cells (GMC, the direct progeny of neuroblasts) divide symmetrically into two distinct neural progeny, they generate neurons that are either *Notch-On* (N^{ON}) or *Notch-Off* (N^{OFF}), forming two distinct 'hemilineages' from a single neural progenitor (Truman et al. 2010) (Figure 1C). Each of these mechanisms during neurogenesis is essential for generating neural diversity in the adult brain. Recently, these mechanisms have been correlated with the assembly of neuronal circuits, implicating a link between neural diversity and neural circuits (Kao et al. 2012; Sen et al. 2014; Pinto-Teixeira et al. 2018; Sullivan et al. 2019). Here, I summarize the genetic manipulations that can rewire the *Drosophila* brain, and propose the central complex of *Drosophila* is an excellent model system to determine basic developmental mechanisms essential for circuit function and animal behavior.

SUMMARY OF ESTABLISHED PRICIPLES

Spatial genes and the assembly of neural circuits

During embryogenesis, neuroblasts express a unique array of transcription factors as they delaminate from the neuroepithelium. Each transcription factor, spatially expressed across both the anterior-posterior and dorsal-ventral body axes, conveys unique molecular information for each neuroblast, establishing the molecular identity of neural progeny generated by each lineage (Skeath and Thor 2003; Urbach and Technau 2004; Technau et al. 2006), a common feature for both vertebrate and invertebrate neural patterning (Reichert and Simeone 2001; Lichtneckert and Reichert 2005; Reichert 2009). Until recently, it was unclear whether these unique genetic programs, which confer progenitor heterogeneity, are also involved in the assembly of complex circuit anatomy and function.

Tens of thousands of neurons within the *Drosophila* central brain emerge from a relatively small pool of ~100 neuroblasts (Truman and Bate 1988; Urbach 2003; Technau et al. 2006). Neurons from the same larval neuroblast lineage often share anatomical and functional features of connectivity by innervating common neuropil regions or axon tracts within the central nervous system (Pereanu 2006; Ito et al. 2013; Lovick et al. 2013; Yu et al. 2013)(Figure 1A). During vertebrate cortical development, neurons that are clonally related commonly innervate the same column or exhibit similar functional properties in response to external stimuli (Yu et al. 2009; Li et al. 2012; Ohtsuki et al. 2012).

Altogether, for both invertebrate and vertebrate species, lineages are correlated with neuronal circuit assembly.

Within the diverse network of adult brain lineages in *Drosophila*, the LALv1 and ALad1 neuroblast lineages are both molecularly and anatomically distinct. LALv1 projects to the central complex, a dense neuropil region associated with adult navigation (Pfeiffer and Homberg 2014), whereas ALad1 projects to the antennal lobe, where olfactory information is processed (Fishilevich and Vosshall 2005). *Sen* et *al.* demonstrate that a single transcription factor, *orthdenticle* (*otd*), is expressed in LALv1 but not ALad1. To define whether *otd* is sufficient to instruct axon pathfinding, and thus, connectivity, the authors first mutate this transcription factor with clonal analysis and determine that mutant LALv1 lineage tracts adopt the same projection pattern as ALad1, and project to the antennal lobe. Conversely, misexpression of *otd* in ALad1 causes a partial reciprocal transformation of connectivity to the central complex. Finally, *otd* clonal mutant LALv1 neurons are functionally integrated into antennal lobe circuitry, and process olfactory information much like ALad1 lineage neurons (Sen et al. 2014). Altogether, these data demonstrate that spatial identity during neurogenesis in the *Drosophila* brain can transform and regulate functional neuronal connectivity, or macro-neuroanatomy (Figure 1A').

Temporal genes and the assembly of neural circuits

Neurons from a common lineage share many features of connectivity, such as innervating a common neuropil structure (Sen et *al.* 2014). Yet within each neuropil structure, there are substructures or targeted regions of innervation, such as glomeruli or layers (Couto et al. 2005; Wolff et al. 2015). It has been shown that *Drosophila* antennal lobe neurons innervate each glomerulus according to their birth-order from a neuroblast lineage (Jefferis et al. 2001). This pioneering study demonstrated that mechanisms regulating neuronal birth-order could correlate with the glomerulus a neuron will innervate. Do neurons encounter different extrinsic cues and environments based on their birth-order, or do intrinsic factors, such as temporal identity genes, instruct circuit assembly? Similarly, mammalian cortical neurons innervate distinct layers of the cerebral cortex based on their birth-order from radial glia progenitors (Molyneaux et al. 2007; Leone et al. 2008). In sum, from vertebrates to invertebrates, precisely timed neurogenesis is potentially a powerful mechanism for determining which substructure neural progeny from a given lineage will innervate. It is unclear, however, whether detailed circuit assembly is caused by birth-time, temporal identity, both, or neither.

Neural progenitors expressing known transcription factors give rise to stereotyped progeny based on birth-order, known as temporal identity. (Kohwi and Doe 2013) (Figure 1B). For *Drosophila,* neuroblasts that generate projection neurons of the antennal lobe express the transcription factor *chinmo* early during larval life (Zhu et al. 2006). When this early temporal transcription factor is mutated from antennal lobe lineages with clonal analysis, neurons that are early-

born target late-born glomeruli in the antennal lobe, thus transforming their glomerulus targeting (Kao et al. 2012) (Figure 1B'). Future work in both *Drosophila* and vertebrate species could determine if this is a universal mechanism across various stages of brain development, rather than a unique feature of the antennal lobe in adult fly.

Notch signaling and the assembly of neural circuits

To assemble functional circuitry coordinating behavior, single neuronal cell types must synapse with specific partners with stringent specificity, conferred by either local guidance cues or synaptic specification molecules (Benson et al. 2001; Betley et al. 2009; Williams et al. 2010). This detailed level of circuit formation is still poorly understood, and the mechanisms are still under heavy investigation. It remains clear that single neuronal cell types position their axons and dendrites in distinct regions of neuropil structures (*e.g.* synaptic targeting). Without these structures, animals are unable to robustly and routinely process complex stimuli (Melnattur and Lee 2011; Zhuang et al. 2017). For example, a recent study discovered that the retinotopic map of the adult *Drosophila* visual system required both temporal patterning and Notch signaling to correctly organize specific lobula cell-type neurons within a circuit map for motion detection (Pinto-Teixeira et al. 2018). T4/T5 motion detection neurons are generated by the same GMC, with $Notch^{OFF}$/ $Notch^{ON}$ generating each subtype, respectively. When Notch-cues are mutated from this GMC, and traced with clonal analysis, both neurons exhibit T4 identity with identical morphology and

targeting (Figure 1C-C'). This study highlights the power of *Drosophila* genetics to uncover simple and basic rules during development that can govern the organization of complex circuit topography.

Current state of the art

Molecular cues that regulate neurogenesis (spatial, temporal, and Notch signaling) correlate with the assembly of neuronal circuits, yet few studies have directly demonstrated that these cues activate genes directly regulating synaptic connectivity, such as cell-surface molecules. One pioneering study discovered that axon trajectory choice in the antennal lobe of *Drosophila* was controlled by both Notch signaling and the subsequent expression of *semaphorin* protein, a cell-surface molecule known for its role in axon guidance (Joo et al. 2013). In this study, Notch mutants were described to have the same antennal lobe axon trajectory choice defects as *semaphorin* mutants, though neither protein was directly linked to synaptic specificity. In order to guide subsequent post-mitotic neurons to their correct neuropil, glomerulus, or synaptic target, spatial or temporal patterning cues could activate similar molecular mechanisms. With the advent of single-cell transcriptomics, these molecular mechanisms could be readily identified and tested in simple nervous systems such as *Drosophila*.

Highlight of future directions

Mechanisms that expand neural diversity during neurogenesis have been well characterized for the last two decades in *Drosophila* and vertebrate species.

Post-mitotic mechanisms that regulate neuronal connectivity have also been well characterized. To date, there are few examples linking these two areas of developmental neuroscience together. Are the mechanisms that regulate molecular diversity also required to regulate neuronal connectivity? It could be that these two areas are independent, and that cell-surface proteins operate only after mitosis. Alternatively, the initial genes activating cell-surface molecule expression could begin with spatial identity, temporal identity, or Notch-signaling during neurogenesis. Future work in relatively simple model organisms, such as *Drosophila*, could yield valuable insights into this emerging area in developmental neuroscience.

Although a direct link between patterning genes and cell surface molecules guiding synaptic specificity remains elusive, many studies highlight the importance of cell-surface molecules in and of themselves for circuit development. Few studies, however, have been able to directly link these factors to circuit function and ultimately to animal behavior (Sullivan et al. 2019). The primary challenge is that behaviors, such as locomotion or vision, are often robust, with redundant or parallel pathways that compensate for minor defects or mutations to single neuronal cell-types. A potential way to overcome these challenges is to investigate behaviors that rely on neural circuit 'bottlenecks' – regions where information flow critical to a particular behavior converges onto a small group of neurons (Olsen and Wilson 2008).

One brain region that will likely prove sensitive to many developmental defects is a highly conserved brain region in arthropods, termed the central

complex (CX), positioned along the midline of the adult brain. The behavioral outputs of this region include path-integration, celestial navigation, sleep, and general sensorimotor transformations (Seelig and Jayaraman 2015; Pimentel et al. 2016; Giraldo et al. 2018). These behaviors are critical for animal survival; they rely on very specific subsets of neurons within the CX, many of which form 'bottlenecks' where information must flow through a single class of neurons (Franconville et al. 2018). Finding the genetic mechanisms required to assemble individual neurons into circuits could disrupt these 'bottlenecks'. Mutations in these pathways will likely yield robust behavioral deficits that can be readily quantified and are independent of basic sensory or motor systems such as vision and locomotion. To that end, in my thesis project, I took advantage of this circuit bottleneck to define the role of the temporal transcription factor *eyeless* in the development of conserved circuit driving celestial navigation (Sullivan et al. 2019).

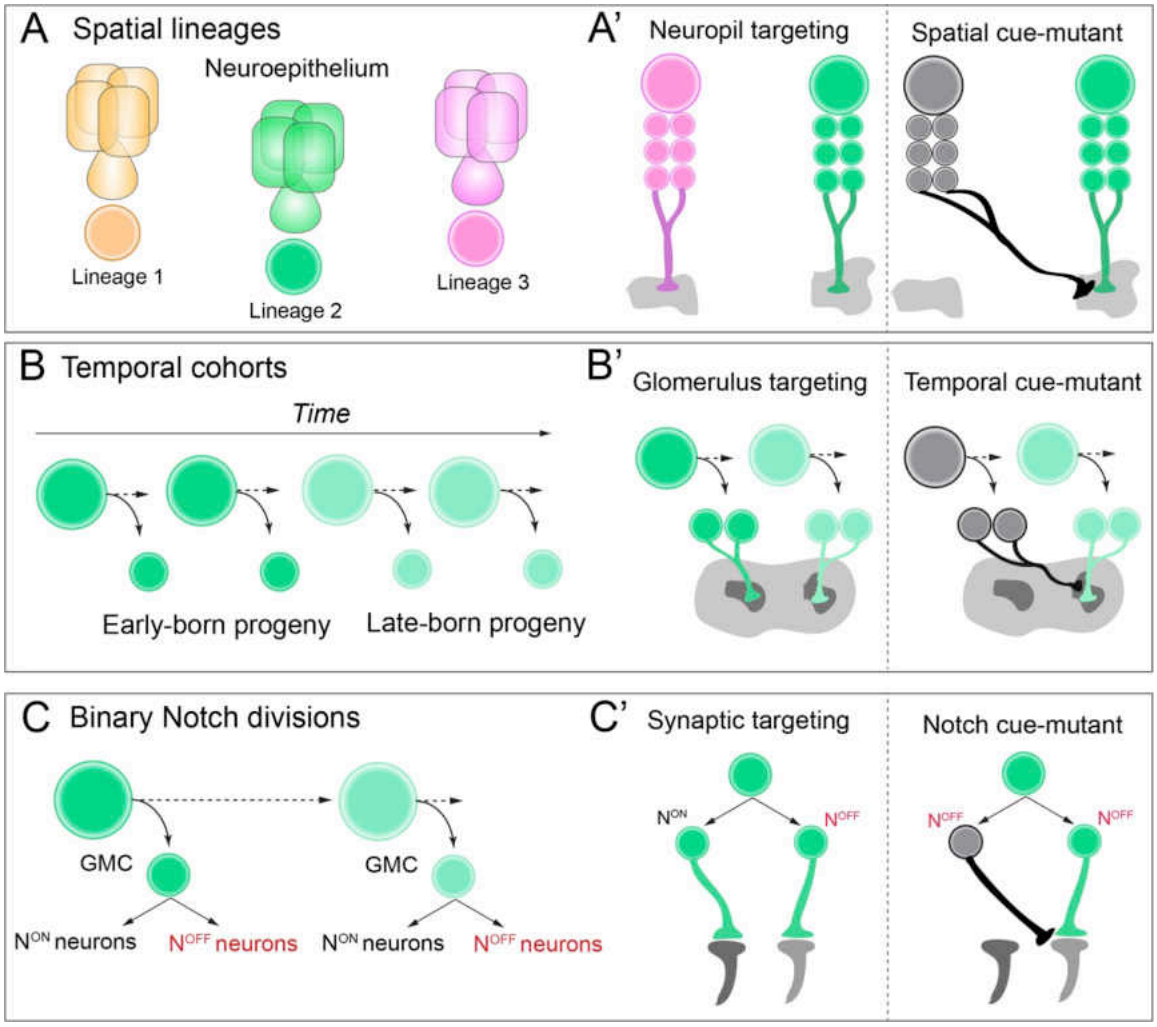

Figure 1. Rewiring the *Drosophila* brain with genetic manipulations in neural lineages. A-A') Neuroblasts acquire a spatial identity based on where they delaminate from the neuroepithelium. Each spatial identity then generates a unique lineage. Each lineage has unique neuropil targeting in the adult central brain of *Drosophila*, and when these spatial identity genes are mutated each lineage, this neuropil targeting can be transformed. B-B') As neuroblasts generate neural progeny and age, they express a series of temporal identity genes, establishing cohorts of neural progeny over time, such as early vs. late born neurons. These neurons have distinct glomerulus targeting in the adult

antennal lobe, and if specific temporal identity genes are mutated, this targeting can be transformed. C-C') As ganglion-mother cells (GMC) divide, they generate two distinct Notch ON vs. OFF 'hemilineages' in the adult brain. These hemilineages can have very distinct synaptic targeting in the optic lobe of *Drosophila*, and if Notch signaling is mutated, their connectivity can be. transformed.

CHAPTER II: TEMPORAL IDENTITY ESTABLISHES CX COLUMNAR NEURONS MORPHOLOGY, CONNECTIVITY, AND FUNCTION

This chapter includes previously published and/or co-authored material. Reproduced with permission from: Sullivan, L. F., Warren, T. L., & Doe, C. Q. (2019) Temporal identity establishes columnar neuron morphology, connectivity, and function in a Drosophila navigation circuit. *eLife*

Work over the past two decades has revealed two important developmental mechanisms that generate neuronal diversity from flies to mice. First, spatial patterning cues produce different pools of neural progenitors (called neuroblasts in insects); second, neuronal progenitors/neuroblasts sequentially express a series of transcription factors that generate additional neuronal diversity (Kohwi and Doe 2013). These so-called “temporal transcription factors” or TTFs are expressed transiently in progenitors, are inherited by neurons born during the expression window, and specify progenitor-specific neuronal identity (Rossi et al. 2016; Doe 2017). For example, the Hunchback (Hb) TTF is present in *Drosophila* embryonic neuroblasts as they produce their first progeny; loss of Hb leads to absence of first-born neurons, whereas prolonging Hb expression generates ectopic first-born neurons (Isshiki et al. 2001). While TTFs are clearly important for generating molecularly distinct neuronal subtypes, their role in establishing neuronal morphology, connectivity, and behavior remains relatively poorly understood.

Recent work has shown that there are only four bilateral “type II” neuroblasts that generate the intrinsic neurons of the central complex (CX)

projecting to the protocerebral bridge (PB). These four neuroblasts are named DM1-DM4 (Yang et al. 2013; Andrade et al. 2018) or DM1-DM3 and DM6 (Riebli et al. 2013); here we use the DM1-DM4 nomenclature (Figure 2A). Type II neuroblasts have a complex lineage. They repeatedly divide every 1.6h to generate a series of molecularly distinct intermediate neural progenitors (INPs), which in turn divide every 2-3h to produce 4-6 molecularly distinct ganglion mother cells (GMCs) that each yield a pair of sibling neurons (Figure 2B) (Bello et al. 2008; Boone and Doe 2008; Bowman et al. 2008; Homem et al. 2013). Several laboratories have identified candidate temporal transcription factors (TTFs) that are expressed in type II neuroblasts, such as the Ecdysone Receptor (EcR) (Figure 2B, horizontal axis; Syed et al., 2017) or in INPs, such as Dichaete and Eyeless (Figure 1B, vertical axis; Bayraktar and Doe, 2013). Each of these TTFs is required to specify the identity of neurons born during its neuroblast or INP expression window (Bayraktar and Doe 2013; Ren et al. 2017; Syed et al. 2017).

In this study we address how larval brain TTFs contribute to the development and function of the adult insect central complex (CX). The CX is a highly conserved brain region in insects that is thought to play a crucial role in navigation and motor control (Pfeiffer and Homberg 2014; Green et al. 2017; Heinze 2017; Kim et al. 2017; Franconville et al. 2018; Green et al. 2018). The CX is characterized by four distinct neuropil regions: the Ellipsoid Body (EB), Fan-shaped Body (FB), Protocerebral Bridge (PB), and Noduli (NO); the CX is also connected to lateral neuropils termed the Gall and the Round body (ROB)

(Wolff et al. 2015). Columnar neurons, which innervate single glomeruli that tile the entire EB and PB neuropil, have been shown to play a key role in navigation (Pfeiffer and Homberg 2014; Green et al. 2017; Heinze 2017; Kim et al. 2017; Turner-Evans et al. 2017; Franconville et al. 2018; Green et al. 2018). There are at least four columnar neuron subtypes (Figure 2C). The E-PG neurons have spiny dendritic arbors in the EB (hence the E at the front of their name) and provide outputs to the PB and Gall (hence the PG at the end of their name); conversely, P-EN neurons have spiny dendritic arbors in the PB and provide outputs to the EB and Noduli. Recently it has been proposed that the E-PG/P-EN neurons form a recurrent circuit that tracks the fly's orientation in space (Lin et al. 2013; Green et al. 2017; Turner-Evans et al. 2017; Green et al. 2018). Two additional columnar neuron classes are PF-R neurons that have dendritic spines in the PB and FB and project axons to the ROB, and the P-FN neurons which have dendritic spines in the PB and project axons to the FB and Noduli (Figure 1A) (Wolff et al. 2015; Wolff and Rubin 2018); both are proposed to have a role in navigation based on anatomical connectivity (Heinze 2017; Wolff and Rubin 2018), but their function has not been experimentally determined.

Here we map the developmental origin of these four CX neuronal subtypes postulated to have a critical role in navigation. We find that each is derived from a specific temporal window during the INP cell lineage, and that neurons with similar developmental origins have similar axon/dendrite neuropil targets. We confirm that Eyeless, previously shown to be a INP TTF (Bayraktar and Doe, 2013), is expressed in the latter half of INP lineages; we go on to show

that Eyeless is required to promote the identity of the two CX neuron subtypes born late in INP lineages (E-PG, PF-R) as well as to repress the identity of the two CX neuron subtypes born during early INP lineages (P-EN, P-FN). In this way, the Eyeless TTF regulates the relative proportion of each neuronal subtype: loss of Eyeless generates fewer E-PG neurons and more P-EN neurons. Importantly, the ectopic P-EN neurons have normal anatomical connectivity. Finally, we show that loss of Eyeless specifically during the larval stages when E-PG neurons are born results in a highly specific defect in adult flight navigation, consistent with the proposed role of E-PGs in maintaining an arbitrary heading to a sun stimulus. Our findings are the first to identify the developmental origin of functionally important adult flight navigation neurons. Moreover, they set the stage for manipulating developmental genetic programs to alter the number and function of each class of adult CX neurons.

Developmental origin of CX columnar neurons

CX columnar neurons are generated by type II neuroblast lineages

We used intersectional genetics to map the developmental origin of four CX columnar types (Scheme 1). Our strategy was to use the FLP enzyme to permanently open a *lexAop-FRT-stop-FRT-GFP* reporter in specific populations of INPs and then use adult columnar neuron LexA transgenes to determine the number of each adult columnar neuron type made by each of these INP populations. This approach allowed us to map the developmental origin of

neurons labeled by LexA reporters only at pupal or adult stages. We opened the *lexAop-FRT-stop-FRT-GFP* reporter in all INPs of the type II neuroblast lineages and confirmed that all four types of adult CX columnar neurons are generated by type II neuroblasts (Scheme 1). Indeed, we found that type II neuroblasts make all 30 PF-R neurons, all 40 E-PG neurons, all 40 P-EN neurons, and all 50 P-FN neurons across both hemispheres of the adult brain (Figure 2D). We conclude that the four types of CX columnar neurons are all derived from type II neuroblast lineages.

CX columnar neurons are generated by young type II neuroblast lineages

The challenge in birth-dating CX neurons from type II neuroblast lineages is that they are generated across two temporal axes, NB and INP. To address this, we systematically dissected one axis at a time. Larval type II neuroblasts produce neurons over five days (0-120h after larval hatching; ALH), with each lineage generating roughly between 40-50 INPs, totaling around 400 neurons and additional glia from each distinct lineage (Homem et al. 2013). We used intersectional genetics to determine when each columnar neuron subtype was born during the type II neuroblast lineage. We transiently expressed the FLP recombinase in INPs to permanently open the lexAop reporter at different times during type II neuroblast lineages and assayed for the number of PF-R, E-PG, P-EN, or P-FN adult neurons made at each time-point (method summarized in Scheme 1B). We found that PF-R neurons were made first in larval type II neuroblast lineages, followed by E-PG neurons, and then by P-EN and P-FN

neurons which share overlapping birthdates (Figure 3A). The relatively broad distribution of columnar neuron birthdates is likely due to DM1-DM4 individual lineages generating neuron subtypes asynchronously, but could also represent natural developmental variation or stochasticity in the time of columnar neuron birthdates; it is most consistent with each pool of 30-50 columnar neurons being generated within a 12h temporal window in the type II neuroblast lineage (Figure 3B).

CX columnar neurons with similar developmental origin have similar axon/dendrite targeting

We next defined columnar neuron birthdates along the INP temporal axis (see Scheme 1C). Young INPs express Sox family transcription factor Dichaete (D), whereas old INPs express the Pax6 family transcription factor Eyeless (Bayraktar and Doe 2013; Eroglu et al. 2014; Farnsworth et al. 2015). Here we test whether columnar neuron subtypes arise from a young D+ or old Ey+ temporal window. As expected, all columnar neuron subtypes are labeled when the lexAop reporter is 'opened' in all INPs (Figure 4A-D). In contrast, when the lexAop reporter is 'opened' only in old INPs, we detect all 40 E-PG and all 30 PF-R adult neurons but no P-EN or P-FN neurons (Figure 4E-H). We conclude that all P-EN and P-FN neurons are born from young INP lineages, whereas all E-PG and PF-R neurons are born from old INP lineages (summarized in Figure 3I). Interestingly, the P-EN and P-FN columnar neurons have a highly similar developmental origin and project to similar CX neuropils (dendrites to PB, axons

to Noduli; Figure 4I), whereas E-PG and PF-R columnar neurons have distinct developmental origins and share no similarities in neuropil targets, suggesting that developmental origin may be tightly linked to neuronal morphology and anatomical connectivity (see Discussion).

Discussion

We have shown that distinct classes of CX columnar neurons have unique developmental origins within type II neuroblast lineages. We find that CX columnar neurons map to four bilateral type II neuroblast lineages (DM1-DM4), confirming previous work (Wang et al. 2014). Thus, per brain there are 8 parental neuroblasts that generate 30-50 neurons of each subtype, or 4-6 neurons per neuroblast. These 4-6 neurons could arise from 2-3 GMCs in a single INP lineage, or as 1 neuron from 6 different INPs; twinspot MARCM would be needed to determine their precise cell lineage. Our birth-dating results indicate that CX columnar neurons originate from distinct INPs born ~12h apart during larval life, except for P-EN and P-FN neurons whose similar birthdates suggest they may arise from the same INPs. Twin-spot MARCM analysis (Lee and Luo 1999) would be necessary to determine whether P-EN and P-FN neurons arise from the same or different INPs. Interestingly, the two CX columnar neurons born at the same time (P-EN and P-FN) have axon projections intrinsic to the CX and target the same neuropils (PB and Noduli). In contrast, the two CX columnar neuron types born at different times (E-PG and P-FR) have axon projections extrinsic to the CX and target different neuropils (Gall and ROB). This raises the

possibility that neuroblast temporal identity determines whether columnar neuron axon projections are intrinsic or extrinsic to the CX. More generally, the results suggest that neurons with similar temporal identity have matching connectivity.

We have mapped the birthdates of only four CX columnar neuron subtypes out of the 60 distinct neuronal subtypes innervating the CX (Young and Armstrong 2010). Mapping these other neurons to their type II neuroblast and INP lineages is an important task for the future, which will help identify developmental correlates of neuronal morphology, connectivity, and function. Additionally, significant neuronal diversity may arise from GMCs dividing to make $Notch^{ON}$/$Notch^{OFF}$ sibling neurons, which often have distinct morphology (Truman et al. 2010; Lacin et al. 2014; Wang et al. 2014; Harris et al. 2015). The role of Notch signaling in generating hemilineages within type II neuroblast progeny remains unexplored.

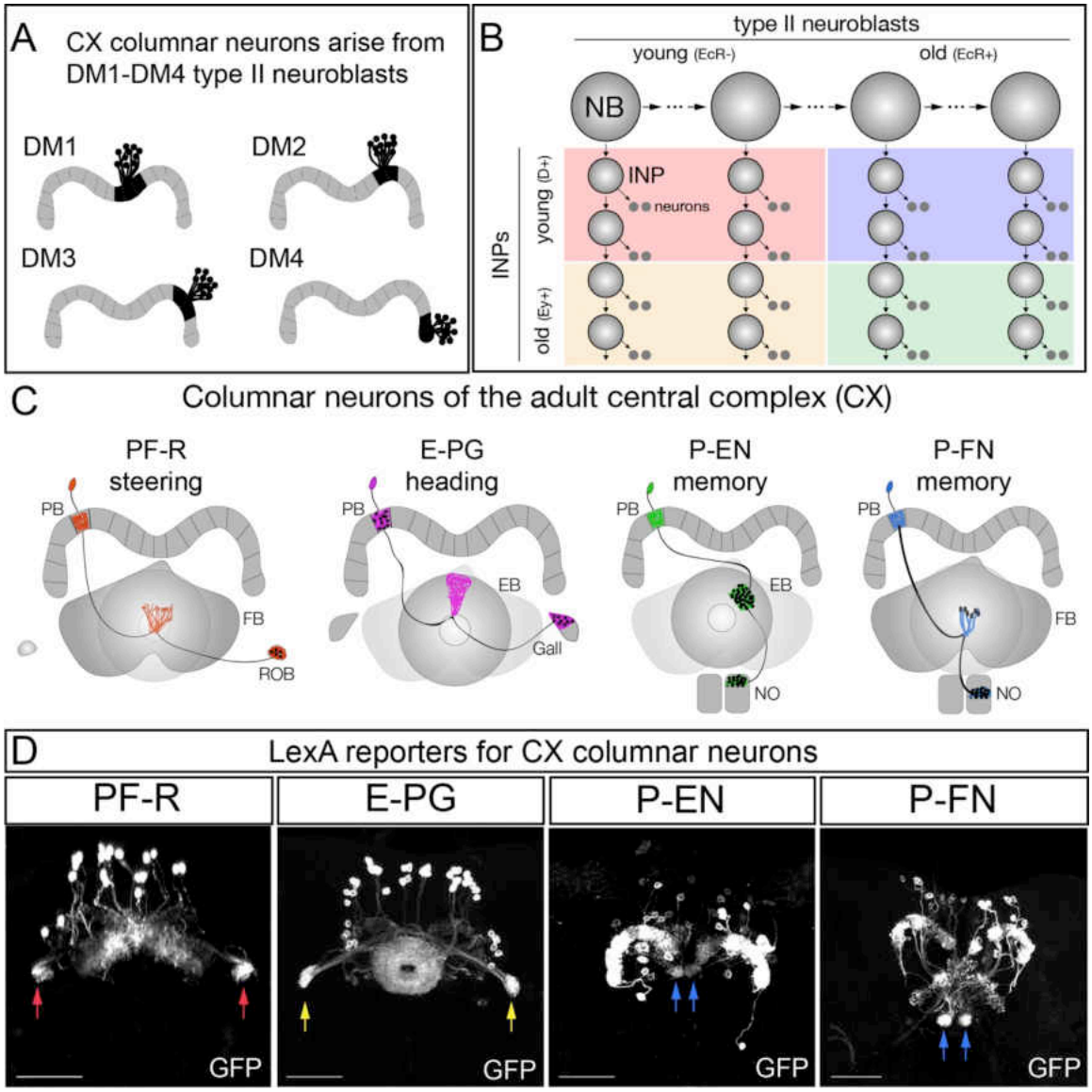

Figure 2. CX columnar neurons are generated by type II neuroblast lineages.

(A) CX columnar neurons innervating the PB originate specifically from each of four bilateral type II neuroblast lineages (DM1-DM4), which includes all four neuronal subtypes shown in panel D. DM1 lineage neurons innervating the most medial PB glomeruli, and DM4 lineage neurons innervating the most lateral PB glomeruli. Adult brain right hemisphere shown.

(B) Type II neuroblasts divide every 1.6h to generate ~60 INPs; each INP progeny divides every 2-3h to produce 10-12 neurons (Homem et al. 2013). Both neuroblasts and INPs express temporal transcription factors that subdivide their lineages into distinct molecular windows. Finer subdivisions exist but are not shown for clarity.

(C) PF-R, E-PG, P-EN, and P-FN columnar neuron subtypes; each has a proposed function in navigation (line 2) and a distinct pattern of connectivity. PB, protocerebral bridge; FB, fan-shaped body; ROB, round body; EB, ellipsoid body; NO, noduli.

(D) Adult CX columnar neurons derived from INPs labeled with adult LexA lines specific for each subtype; See Scheme 1A for genetic details. ROB, red arrows; Gall, yellow arrows; Noduli, blue arrows. Scale bars, 40μm. Genotypes: PF-R, *UAS-FLP; R9D11-Gal4, R37G12-lexA; lexAop(FRT.stop)mCD8::GFP;* E-PG, *UAS-FLP; R9D11-Gal4, R60D05-lexA; lexAop(FRT.stop)mCD8::GFP;* P-EN, *UAS-FLP; R9D11-Gal4, R12D09-lexA; lexAop(FRT.stop)mCD8::GFP;* P-FN, *UAS-FLP; R9D11-Gal4, R16D01-lexA; lexAop(FRT.stop)mCD8::GFP.*

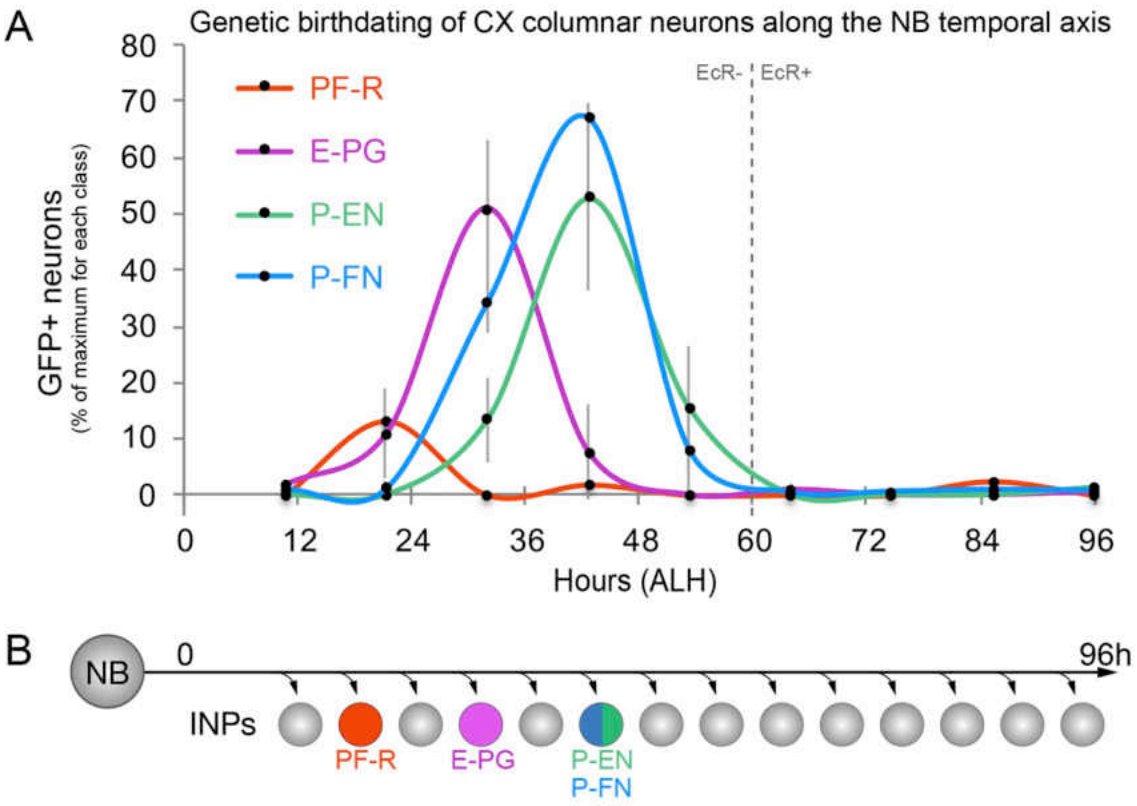

Figure 3. CX columnar neurons are generated by young type II neuroblast lineages.

(A) Identifying the time during the neuroblast lineage that produces each columnar neuron subtype. See Scheme 1B for genetic details. Note that PF-R neurons are born first, E-PG neurons second, and then P-EN/P-FN neurons sharing a common birthdate (n=3-6 per time-point).

(B) Summary of NB birthdating results.

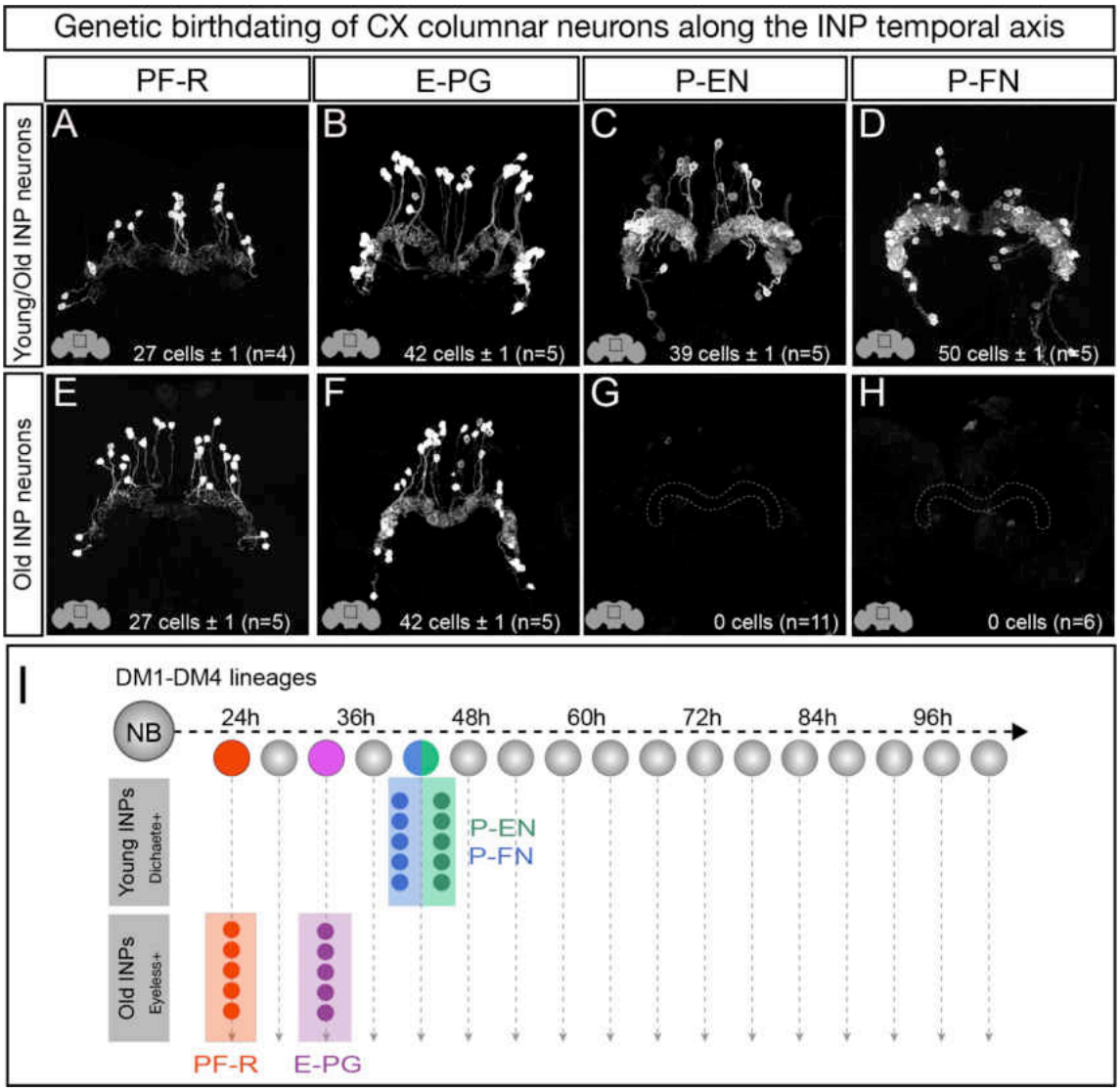

Figure 4. Each CX columnar neuron type arises exclusively from young or old INP lineages.

(A-D) Columnar neuron cell bodies labeled by subtype-specific LexA lines derive from INP lineages (n=5 for each experiment). Staining shows the volume containing cell bodies; thus most axon and dendrite projections are not visible. See Scheme 1A for genetic details.

(E-H) The PF-R and E-PG columnar neurons are generated by late INPs (n=5 for each experiment), whereas the P-EN (n=11) or P-FN (n=6) neurons were not

derived from old INPs and thus are fully derived from young INPs. Staining shows the volume containing cell bodies; thus most axon and dendrite projections are not visible. See Scheme 1C for genetic details.

(l) Summary of INP birthdating results.

Specification of CX Columnar Neurons

The Eyeless temporal transcription factor promotes E-PG and PF-R molecular identity

Our birthdating results indicated that INP age might be a major determinant of CX columnar neuron morphology and connectivity. We next tested whether the TTF Eyeless, which is expressed by INPs during the last half their lineage, specifies the identity of PF-R and E-PG neurons, which are born from Ey+ INPs. To knock down Eyeless expression in INPs, we used an *eyeless* enhancer-Gal4 line (*R16B06-Gal4*) that is expressed in old INPs (Farnsworth et al. 2015) to drive a *UAS-Ey*^{RNAi} transgene that we previously showed eliminates all detectable Eyeless protein (Bayraktar and Doe 2013).

In wild type adults, there are ~40 E-PG neurons and ~30 PF-R neurons (Figure 5A,B; quantified in G,H). In adults where Ey^{RNAi} is expressed in old INPs, we found nearly complete loss of PF-R and E-PG neurons (Figure 5D,E; quantified in G,H); we suggest that these neurons are converted into an early-born INP progeny identity (for which we have no markers), but we can't rule out that they undergo apoptosis. In addition, we performed an antibody screen for neuronal markers of CX neuronal subtypes, and identified Toy as specifically

marking all of the old INP-derived PF-R and E-PG neurons but none of the young INP-derived P-EN and P-FN neurons. Here we show that Toy+ neurons generated by old INPs are also significantly reduced following Ey^{RNAi} in old INPs (Figure 5C,F; quantified in I). We conclude that the Eyeless temporal transcription factor is required for the specification of PF-R and E-PG columnar neurons.

The Eyeless temporal transcription factor represses P-EN and P-FN molecular identity

The P-EN and P-FN columnar neurons derive from early INP progeny, prior to the expression of Eyeless in later-born INPs, raising the question of whether Eyeless expression triggers a switch from early-born P-EN/P-FN production to late-born E-PG/PF-R production. To determine if Eyeless terminates production of early-born P-EN and P-FN columnar neurons, we expressed Ey^{RNAi} in old INPs, and assayed for ectopic P-EN or P-FN neurons. In wild type adults, there are ~40 P-EN neurons and ~50 P-FN neurons (Figure 6A,B; quantified in G,H). In adults where Ey^{RNAi} was expressed in old INPs, we found an over two-fold increase in the number of P-EN and P-FN neurons (Figure 6D,E; quantified in G,H). In addition, the antibody screen described above identified the transcription factor Runt as specifically marking all early-born P-EN and P-FN neurons but none of the late-born E-PG and PF-R neurons (data not shown). In wild type, there are ~220 Runt+ adult neurons made by INP progeny, but Ey^{RNAi} led to a significant increase to ~580 Runt+ adult neurons

(Figure 6C,F; quantified in I), consistent with a role for Eyeless in terminating production of young INP-derived neurons. We conclude that Eyeless maintains equal pools of E-PG and P-EN neurons by triggering a switch from early-born P-EN/P-FN neurons to late-born E-PG/PF-R neurons.

Discussion

By mapping the developmental origins of four classes of columnar neurons innervating the central complex, we find that each class derives from a relatively tight window during the neuroblast lineage, and from either young or old INPs (Figure 3I). The fact that all of the four subtypes are restricted to early or late in the INP lineage suggests that the early/late lineage distinction is developmentally important, consistent with our finding that early/late INPs express different TTFs (Dichaete/Eyeless, respectively). Furthermore, mapping the lineage of each neuronal class allowed us to identify a correlation with developmental origin and neuronal morphology (neurons with similar birth-dates have similar morphology). Many other developmental windows have yet to be characterized, for example the neurons derived from young INPs prior to PF-R/E-PG production are unknown, and would be expected to be expanded in the absence of Eyeless; similarly, the neurons derived from the old INPs following production of the P-EN/P-FN neurons are unknown, and would be expected to be missing in the absence of Eyeless. We tested Dichaete and Grainy head for a role in specification of early INP-derived P-EN and P-FN neurons, but observed no phenotype (data not shown); this is unsurprising for Grainy head, because it is

not expressed in the DM1 lineage (Bayraktar and Doe, 2013) which generates P-EN and P-FN neurons. In the future, our intersectional genetic approaches can be used to map the developmental origin of any neuronal subtype for which there exists an adult LexA driver line. For example, we have recently mapped the CX dorsal fan-shaped body “sleep neurons” (Donlea et al. 2011; Ueno et al. 2012; Dubowy and Sehgal 2017; Donlea et al. 2018) to an old neuroblast developmental window (M. Syed, LS, and CQD, unpublished).

We have shown that Eyeless maintains a balance of early-born P-EN/P-FN neurons and late-born E-PG/PF-R neurons by triggering a switch from early-born to late-born neuronal identity. Loss of Eyeless generates fewer E-PG neurons and more P-EN neurons (Figures 5,6). We document the loss of late-born E-PGs here, but many other uncharacterized neurons are also likely to be lost, except during our heat pulse experiments where we tried to specifically target E-PG neurons (Figure 9). Similarly, we document the production of ectopic P-EN neurons in the absence of Eyeless, but many other early-born neuron populations are likely to be expanded. We considered performing clonal analysis to identify the neurons sharing an INP lineage with our four neural subtypes, but decides against it because INPs make morphologically different neurons at each division (Wang et al. 2014); we would not be able to map these neurons to early or late in the INP lineage, nor would we have molecular or genetic markers for these neurons. Determining the identity and birth-order of neurons within each INP lineage will be a difficult task for the future. Developing markers for the remainder of the 60+ different CX neuronal subtypes will be needed understand

the breadth of Eyeless function in generating CX neuronal subtypes. Additional neuronal subtype markers will also be important to test the role of type II neuroblast candidate TTFs (Ren et al. 2017; Syed et al. 2017). We predict that at least some of these candidate TTFs will be required to specify the identity of the four columnar neuron classes described here.

We were interested in whether misexpression of Eyeless in young INPs was sufficient to induce ectopic late-born PF-R and E-PG neurons. We could not simply use *R9D11-Gal4* to misexpress Eyeless in young INPs, because we previously showed that in this genotype Ey translation is repressed in young INPs (Farnsworth et al. 2015). Thus, we permanently expressed Eyeless in INPs and their progeny (*R9D11-FLP, actin-FRT-stop-FRT-Gal4 UAS-eyeless*) but observed loss of all four neuronal subtypes (data not shown). Our interpretation is that permanent high level expression of Eyeless in INPs and their progeny leads to neuronal death, although we can't rule out that Ey transforms all INP progeny into a late-born cell type that we lack markers to detect.

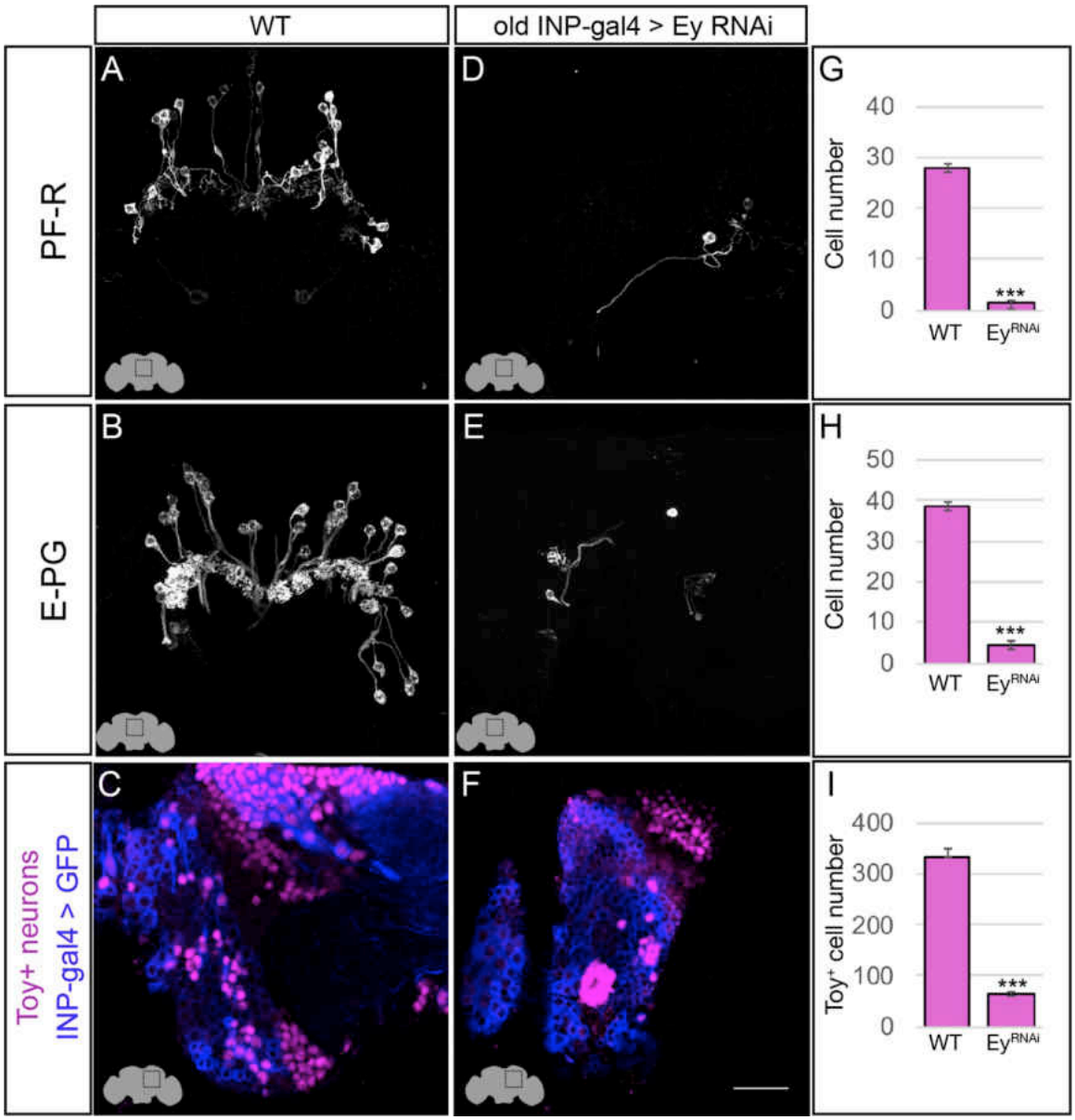

Figure 5. Eyeless promotes PF-R and E-PG molecular identity.

(A-C) Wild-type numbers of PF-R, E-PG, and Toy^{+} neurons in the dorsoposterior adult brain. PF-R and E-PG neurons detected by expression of neuron-specific LexA lines. See methods for genotypes.

(D-F) Eyeless^{RNAi} in INP lineages decreases the number of PF-R, E-PG, and Toy^{+} late-born neurons in the dorsoposterior adult brain. See methods for genotypes.

(G-I) Quantification (n=5 for each experiment). ***, p <0.001. Scale bar, 20μm

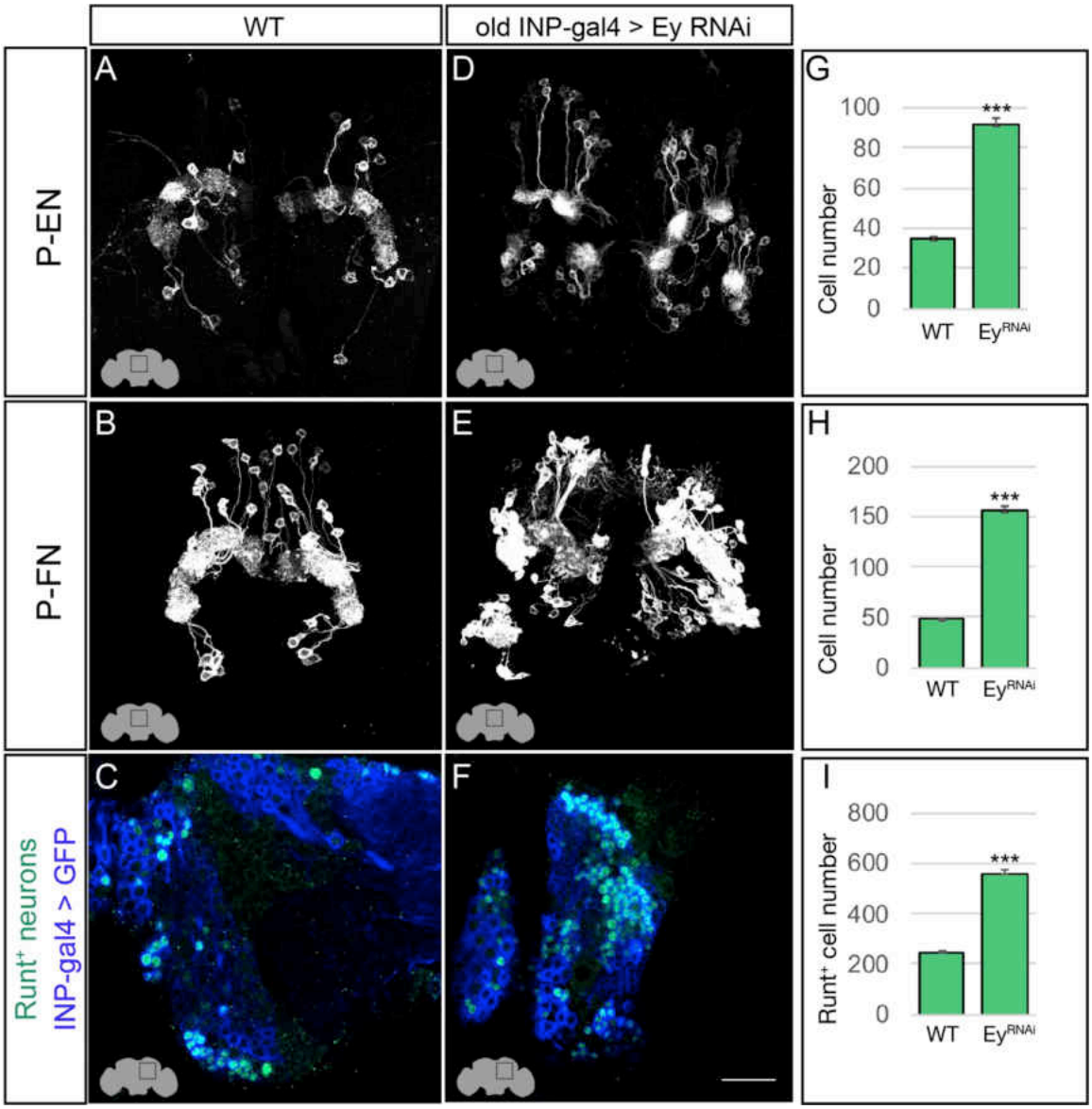

Figure 6. Eyeless represses P-EN and P-FN molecular identity.

(A-C) Wild-type numbers of P-EN, P-FN, and Runt^{+} neurons in the dorsoposterior adult brain. P-EN and P-FN neurons detected by expression of neuron-specific LexA lines. See methods for genotypes.

(D-F) Eyeless^{RNAi} in INP lineages increases the number of P-EN, P-FN, and Runt^{+} late-born neurons in the dorsoposterior adult brain. See methods for genotypes.

(G-I) Quantification (n=5 for each experiment). ***, p <0.001. Scale bar, 20μm

Determinants of Connectivity in CX Columnar Neurons

Loss of Eyeless produces ectopic P-EN neurons with endogenous P-EN morphology and anatomical connectivity

Loss of Eyeless extends the production of P-EN neurons into an older stage of INP lineages, creating a mismatch between their molecular temporal identity (early) and their time of differentiation (late). We tested whether the ectopic P-EN neurons have a neuronal morphology and anatomical connectivity characteristic of the endogenous early-born neurons, or whether their later birthdate results in different morphology or connectivity. We designed a genetic method for specifically labeling the ectopic late-born P-EN neurons – but not the endogenous early-born P-EN neurons – to trace their morphology and anatomical connectivity (Scheme 1D).

As expected, control RNAi did not result in any ectopic P-EN neurons, although there were a few neurons labeled outside the central brain and a small pattern of fan-shaped body neurons (Figure 7A-A'''). In contrast, Eyeless^{RNAi} specifically in old INP progeny resulted in the formation of sparse populations of "late-born" ectopic P-EN neurons with projections into the PB, EB, and Noduli (Figure 7B-B'''). These are the same neuropils targeted by wild type early-born P-EN neurons. We conclude that ectopic late-born P-EN neurons have morphology indistinguishable from the normal early-born P-EN neurons (Videos 1-2).

To determine if the ectopic P-EN neurons have the same anatomical connectivity as the endogenous P-EN neurons, we expressed the pre-synaptic active zone marker Bruchpilot (Brp) specifically in the ectopic P-EN neurons. We found that ectopic P-EN neurons localized Brp to the EB and Noduli, but not to the PB. This is the precisely the same as wild type P-EN neurons (Figure 7C-C', summarized in Figure 7E). Furthermore, the ectopic P-EN neurons assemble into proper columns between glomeruli in the PB and tiles in the EB, precisely matching the morphology of endogenous P-EN neurons (Figure 7D; compare to Wolff et al., 2015, Figure 8D1). Thus, ectopic P-EN neurons match the normal early-born P-EN neurons in molecular identity (R12D09-LexA+), morphology (PB, EB, Noduli projections), and anatomical connectivity (Brp puncta in EB and Noduli). Finally, we assay the morphology of the ectopic P-FN neurons following Eyeless^{RNAi}. We find that the expanded pool of P-FNs all innervate the FB and NO, identical to endogenous P-FN neurons, resulting in an enlarged FB and NO (data not shown). We conclude that reducing expression of the TTF Eyeless leads to a doubling of P-EN and P-FN neurons in the CX, which all have proper neuropil targeting. This shows that neuronal birth-date can be uncoupled from neuronal morphology, because we see P-EN and P-FN neurons born later than normal in the INP lineage, yet they establish morphology that mimics that of the endogenous, early-born P-EN and P-FN neurons (data not shown).

The Eyeless target gene Toy is required for E-PG axonal connectivity to the Gall

The TTF Eyeless is required to specify E-PG neuronal identity, but Eyeless does not persist in adult E-PG neurons, raising the question: What Eyeless target genes regulate E-PG connectivity and function? We focused on Twin of eyeless (Toy) which encodes a transcription factor whose expression is induced by Eyeless in old INPs (Bayraktar and Doe 2013) and is maintained in their adult post-mitotic neuronal progeny. We used two previously characterized Gal4 drivers (Kim et al. 2017; Lovick et al. 2017) to express *UAS-toy*^{RNAi} specifically in post-mitotic E-PG neurons at different stages in development and confirmed that it removes all detectable Toy protein (data not shown).

We next determined if depleting Toy in post-mitotic larval E-PG neurons using *R19G02-Gal4 UAS-toy*^{RNAi} altered E-PG survival or morphology. Loss of Toy had no effect on E-PG neuronal number (n=5, p=0.92) or on connectivity to the EB and PB (data not shown). In contrast, we observed greatly diminished E-PG axonal connectivity to the Gall, where in some cases the E-PG projections appeared nearly absent (n=12, Figure 8A-C). We next removed Toy later, beginning ~24h after pupal formation using *ss00096-Gal4 UAS-toy*^{RNAi}, and observed no effect on E-PG neuronal number (n=5, p=.48) or projections to the EB, PB, or Gall (n=6, Figure 8D-F). Surprisingly, however, loss of Toy produced a significant reduction in the levels of the pre-synaptic active zone marker Bruchpilot (Brp) in the Gall (Figure 8G-I). We conclude that Toy is required during larval stages for E-PG connectivity to the Gall, and is required in pupal stages for establishing or maintaining Brp levels at the E-PG axonal terminals in the Gall.

To determine how the loss of Toy during pupal stages affects CX function, we tested whether reduction of Toy in the E-PGs affected sun navigation. We observed no significant change in flies' heading distribution in relation to the sun stimulus, or in the degree to which they stabilized the sun stimulus (data not shown). Therefore, the loss of Toy in pupal E-PG neurons and the associated reduction of Brp at E-PG axon terminals has no discernible effect on sun navigation.

Discussion

We have shown that the ectopic P-EN neurons formed due to reduced Eyeless levels have morphology and anatomical connectivity that matches the endogenous P-EN neurons (i.e. Brp+ neurites to the EB and NO, and Brp-negative neurites to the PB)(Figure 7). It is unknown, however, whether these ectopic P-ENs are functionally connected to the normal P-EN circuit partners. This could be resolved through functional imaging experiments testing whether ectopic P-ENs receive the innervation from E-PG or delta7 neurons like endogenous P-ENs (Franconville et al. 2018) or whether they form functional inputs to known E-PG downstream neurons (Lin et al. 2013; Green et al. 2017; Turner-Evans et al. 2017). Furthermore, we demonstrate that the Eyeless target gene Toy is required for E-PG axonal connectivity to the Gall. Future work could elucidate the target genes of Toy through RNA-seq that are required for assembling this connectivity, such as downstream cell surface molecules, thus

linking INP temporal identity to a direct mechanism for neuronal connectivity in a highly conserved adult brain region.

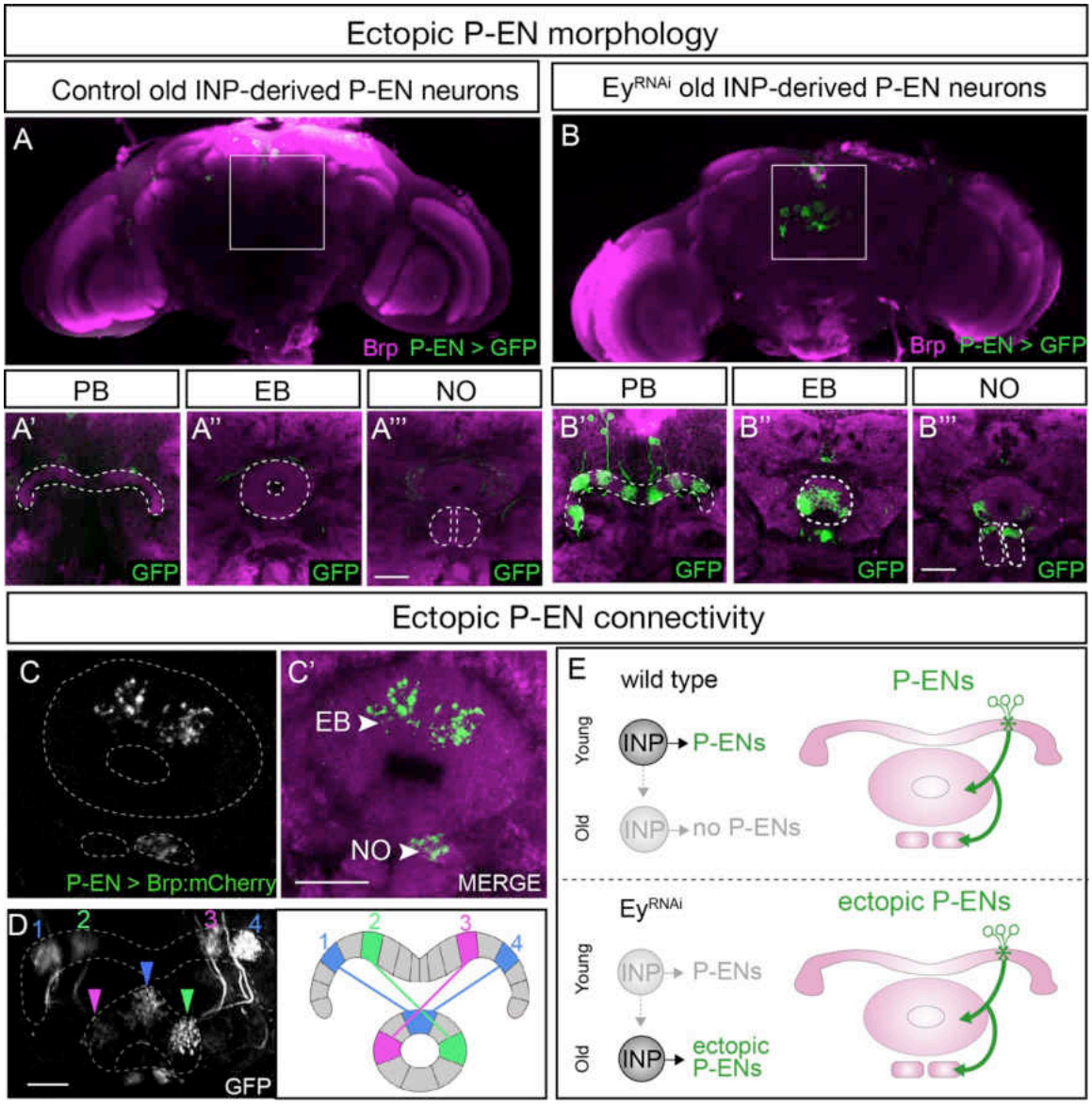

Figure 7. Eyeless^{RNAi} produces late-born 'ectopic' P-EN neurons that have normal P-EN morphology and connectivity.

(A-A’’’) In wild-type adults, late INP clones do not label P-EN neurons in the adult brain (n=5). See methods for details. PB, EB, and NO neuropils marked with dashed lines. Scale bars, 20mm (A-B).

(B-B’’’) In Eyeless^{RNAi} adults, late INP clones produce ectopic late-born P-EN neurons, which project to the PB, EB, and Noduli (n=5), similar to endogenous P-EN neurons (Figure 1A,B). See methods for details. PB, EB, and NO neuropils marked with dashed lines.

(C-C’) In Eyeless^{RNAi} adults, late INP clones produce ectopic late-born P-EN neurons, which localize the pre-synaptic marker Brp::mCherry to the EB and Noduli (n=5), but not the PB (not shown), similar to the endogenous P-EN neurons. Scale bars, 20mm (C-D).

(D) Eyeless^{RNAi} adult, showing stochastic labeling of four ectopic P-EN neurons (1-4) with normal PB and EB glomeruli targeting (compare to Wolff et al., 2018 Figure 8D1). See methods for details.

(E) Summary.

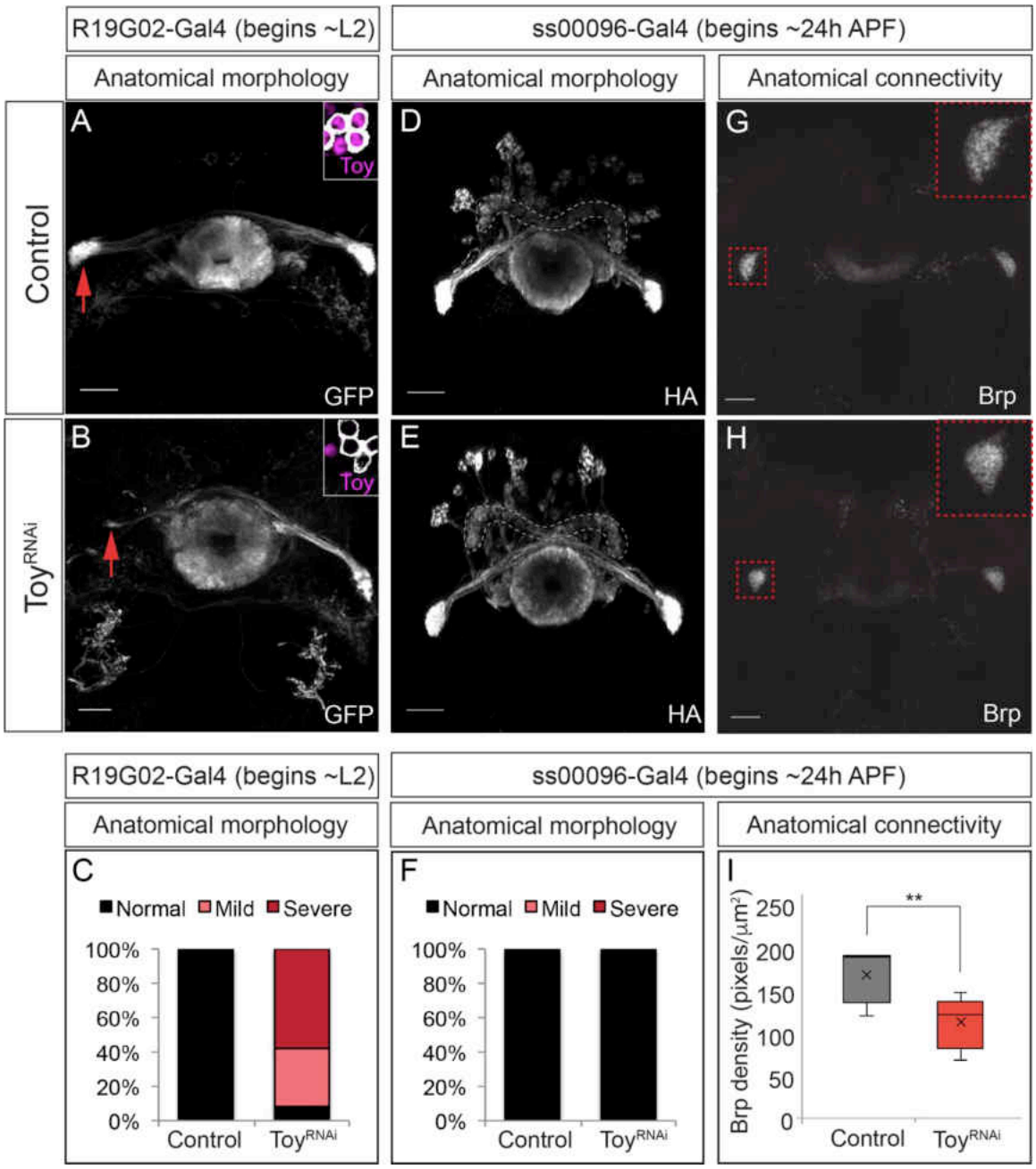

Figure 8. The Eyeless target gene Toy is required for E-PG axonal connectivity.

(A-C) Loss of Toy in larvae reduces E-PG projections to the Gall in adults. (A) Wild type: *R19G02-Gal4* is first expressed at ~L2 and labels adult E-PG neurons;

note projections to the EB (center) and Gall (left and right); PB, not shown (n=6). Inset shows WT levels of Toy-protein expression. (B) *R19G02-Gal4 UAS-Toy^{RNAi}* reduces E-PG projections to the Gall (red arrow), yet projections to the EB and PB (not shown) remain intact (n=12). Inset shows loss of Toy-protein expression. Quantification: mild, detectable reduction in the Gall in one hemisphere; severe, virtually complete loss of Gall. (D-F) Loss of Toy in pupae has no effect on E-PG projections. (D) In wild type, *ss00096 split-Gal4* is expressed ~24h after pupal formation and labels adult E-PG neurons; n=5. (E) *ss00096 split-Gal4 UAS-Toy^{RNAi}* adults have normal projections to the EB (center), Gall (left and right), and PB (outlined); n=5. (F) Quantification. (G-I) Loss of Toy in pupae reduces pre-synaptic levels of Brp in the Gall.

(G,H) Genotypes as in D-E, showing that the pre-synaptic marker Brp is reduced in the E-PG axons targeting the Gall following ToyRNAi (n=6). (I) Quantification. Scale bars, 20mm.

The Effects of Eyeless Manipulation on Navigation Behavior

Transient Eyeless reduction impairs adult flight navigation behavior

Our finding that the temporal transcription factor Eyeless contributes to the development of CX columnar neurons raises the question of how Eyeless influences CX function. Recent work has shown that silencing adult E-PG neurons impairs flies' capacity to maintain an arbitrary heading to a bright spot resembling the sun (Giraldo et al. 2018; Green et al. 2018), a finding that we independently confirmed (data not shown). Based on these results, we hypothesized that Eyeless function during development may be required for adult E-PG function in sun navigation. To reduce Eyeless expression, we drove Eyeless^{RNAi} in old INPs using *R16B06-Gal4*. Temporal control over Eyeless^{RNAi} was achieved with the temperature-sensitive Gal4 inhibitor Gal80. We raised animals at the Gal80 permissive temperature (18^{o}C) to prevent Eyeless^{RNAi} expression and shifted to the non-permissive temperature (29^{o}C) for 24h at the time E-PG neurons are born and differentiate (Figure 9A). Both control and Eyeless^{RNAi} animals exposed to this regime had no major morphological defects in the central complex (Figure 9B,C; data not shown), indicating that E-PG neuron number is likely normal (see Discussion). We then examined how the transient reduction of Eyeless in larval INPs affected the ability of adult flies to maintain an arbitrary flight heading to a fictive sun (Figure 9D). We compared the sun headings of Eyeless^{RNAi} flies that received the 29^{o}C heat pulse with two control groups. One control group had an identical genotype but received no heat pulse (Figure 7E). A second control group received the heat pulse but

Eyeless^{RNAi} was replaced with mCherry ^{RNAi} (Figure 9F). In both control groups, we found that flies maintained arbitrary headings, as expected, with a slight bias towards headings where the sun was behind the fly (Figure 9E,F,I). In contrast, flies with transient Eyeless^{RNAi} during E-PG development exhibited a marked frontal bias in their heading distribution, which was significantly more frontal than the control distributions (Figure 9G, I; $p<0.01$, permutation test). The control distributions were not significantly different from each other ($p=0.49$). Notably, although the heading distributions were distinct, the degree of stimulus stabilization – quantified by calculating the overall vector strength of each flight - was equivalent in the Eyeless^{RNAi} genotype and controls (Figure 9H). Moreover, the Eyeless^{RNAi} genotype and controls showed equivalent performance orienting to a dark vertical stripe (data not shown), similar to the effect of silencing adult E-PG neurons (Giraldo et al. 2018; Green et al. 2018). This suggests that E-PG silencing and Eyeless^{RNAi} induce similar, relatively specific navigation deficits rather than a more general deficiency in visual-motor flight control. Taken together, our results indicate that a transient loss of Eyeless specifically in old INPs causes specific deficits in adult flight navigation to that of silencing E-PG neurons. Our findings therefore demonstrate the importance of Eyeless for CX function.

Discussion

We found that reducing Eyeless expression during early development (24-48 h after larval hatching) causes a profound shift in how flies orient their flight

relative to a fictive sun stimulus. Whereas control populations adopt a broad set of headings, with a slight bias for orientations where the sun is behind (Figure 9E,F,I), Eyeless^{RNAi} flies choose flight directions where the sun is in front (Figure 9G, I). A similar shift to a more frontal heading distribution occurs when E-PG neurons are silenced, either following expression of the Kir2.1 inward rectifying channel (Giraldo et al., 2017) or with a synaptic transmission blocker in walking flies (Green et al., 2018). The consistent shift to a frontal heading after both E-PG silencing and Eyeless^{RNAi} suggests that Eyeless^{RNAi} affects navigation behavior via perturbation of E-PG neurons, although we cannot rule out an effect on unknown late-born neurons. Eyeless^{RNAi} causes no gross deformities in the CX, suggesting E-PGs were not eliminated by Eyeless^{RNAi} using this regime, as loss of all E-PG neurons produces severe EB defects (Xie et al. 2017). The developmental defects in E-PG neurons could be misexpression of ion channels or other functionally important molecules, rather than apoptosis. In contrast, genetic silencing likely affects all E-PG neurons (Giraldo et al. 2018). The fact that similar behavioral effects are induced by our more subtle Eyeless manipulation and E-PG silencing suggests that sun navigation is highly dependent on E-PG neuron activity. One difference between the behavioral effects of Eyeless^{RNAi} and E-PG silencing is the degree to which flies stabilize the sun stimulus. Whereas silencing E-PG neurons significantly reduces the overall vector strength, a measure of the heading consistency within a flight (Giraldo et al., 2017; Green et al., 2018), there is no such reduction in vector strength in Eyeless^{RNAi} flies (Figure 9H). This difference could be due to the more limited

scope of the Eyeless manipulation or it could reflect some capacity of the adult CX to compensate for the larval developmental defect. Taken together, our findings demonstrate that a specific navigation behavior – arbitrary orientation to a sun stimulus – depends on the precise expression and function of the Eyeless TTF during larval development. These results raise the question of how other types of navigation depend on the development and function of other CX neuronal subtypes.

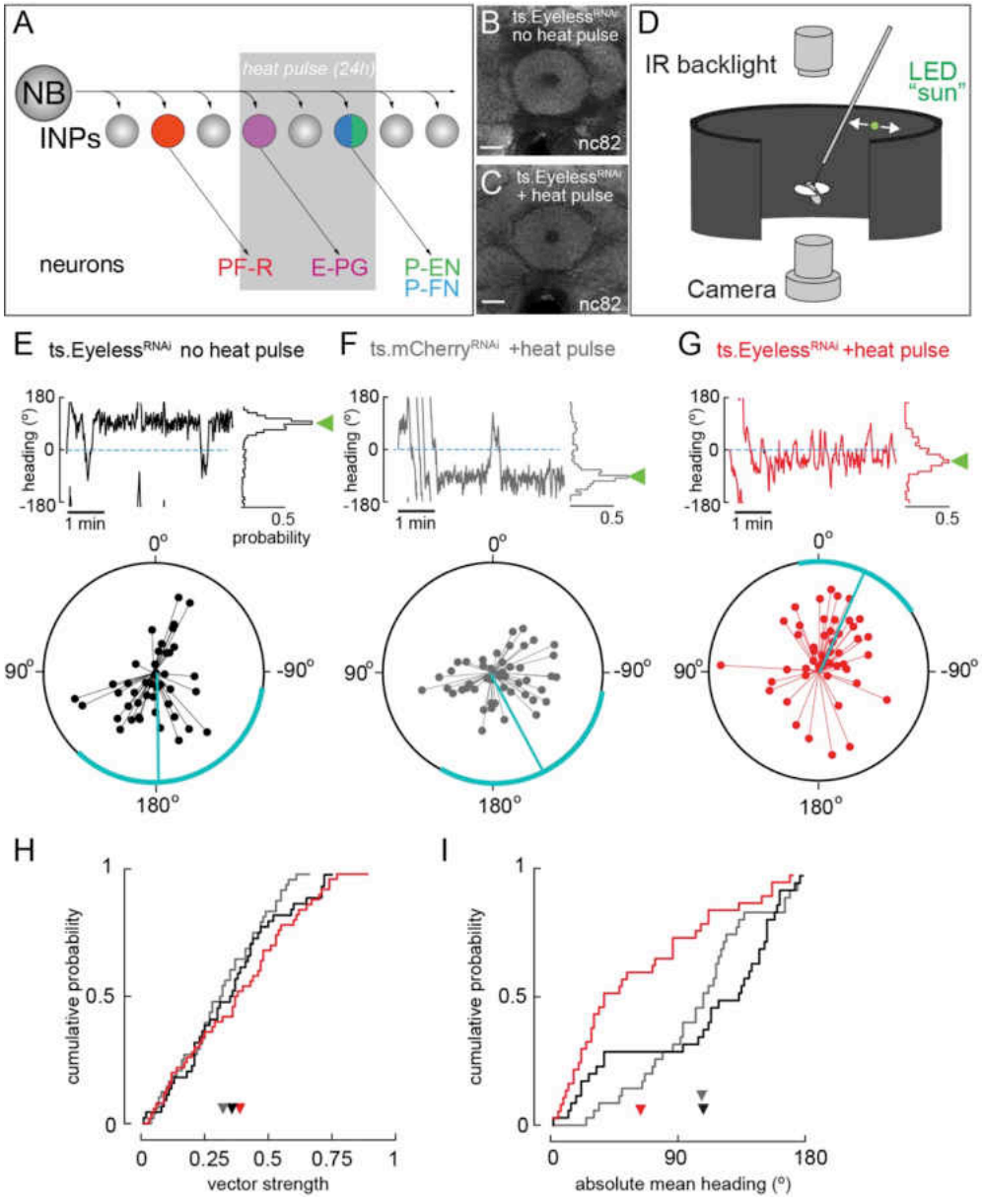

Figure 9. Transient loss of Eyeless during development impairs adult fly navigation.

(A) Timing of Eyeless reduction in INP lineages. Transient inactivation of ts.Gal80 (29°C heat pulse; gray bar) results in transient Eyeless^{RNAi} during the time in which E-PG neurons are normally generated.

(B,C) The manipulation in A does not alter CX neuropil morphology as seen by nc82 (neuropil) staining (EB, shown; other neuropils, data not shown).

(D) Schematic of experimental apparatus for sun navigation experiments. The wing stroke amplitudes of a tethered, flying fly were monitored with an IR camera; the stroke difference determined the angular velocity of a 2.4° sun stimulus. Modified from (Giraldo et al. 2018).

(E) Example flight (top panel) and summary data (bottom panel) from ts.Eyeless^{RNAi} control with no heat pulse. Top panel: left plot shows headings over 5 min flight; 0° is sun position in front of fly. Right histogram is distribution of headings in this example flight; sideways green triangle is the mean. Bottom panel: summary data, with each 5 min flight represented by radial lines. The angle of each line is the mean flight heading. The length of each line is vector strength of flight, varying from 0 (center of circle; no stimulus stabilization) to 1 (edge of circle; perfect stabilization). Each fly flew for two 5 min flights separated by a 5 min rest period. Cyan line shows mean heading, across flights with vector strength>0.2, as well as 95% confidence interval, calculated via resampling across flies. 44 flights, 22 flies total.

(F) Example and summary data from ts.mcherry^{RNAi} control. Same plotting convention as (E). 48 flights, 24 flies.

(G) Example and summary data from ts.Eyeless^{RNAi} flies with heat pulse. Same plotting convention as (E,F). 50 flights, 25 flies.

(H) Cumulative probability distribution of vector strengths from both control groups (black and gray) and from experimental group (red). There was no

significant difference between means (ts.Eyeless^{RNAi} heat pulse, 0.34, red; ts.Eyeless^{RNAi} no heat pulse, 0.31,black;ts.mcherry^{RNAi} heat pulse 0.30,gray; $p>0.1$, permutation test).

(l) Cumulative probability distribution of mean absolute headings. The heading distribution for the experimental group, ts.Eyeless^{RNAi} heat pulse, was skewed significantly to frontal headings (mean 63.7°, 37 flights in 23 flies with vector strength>0.2) compared to control distributions ($p<0.01$, permutation test; ts.Eyeless^{RNAi} no heat pulse, mean 107.9°, 35 flights in 19 flies; ts.mcherry^{RNAi}, mean 106.9°, 31 flights in 21 flies). Scale bars, 10mm.

CHAPTER III: CONCLUSION

In this dissertation, I show that central complex (CX) neurons originate from type II neuroblast lineages in discrete temporal windows. I discovered that neurons with a similar developmental origin have similar axon/dendrite targeting in the CX. Furthermore, I correlate the birth-order of single cell types in the CX with the expression of two temporal transcription factors: *Dichaete* in young INPs and *Eyeless* in old INPs. From here, I demonstrate that *Eyeless* is required to generate or to repress the generation of specific neuronal cell-types in the CX. Additionally, by manipulating *Eyeless* expression in old INPs, I can predictably transform connectivity in the CX through cell-type conversions. Finally, I show that *Eyeless* expression in a discrete developmental window is required for celestial navigation in adult flies, and that the target gene of *Eyeless*, *Toy*, is required for E-PG neuronal connectivity to the gall. Ultimately, this is amongst the first results linking a temporal transcription factor to neuronal connectivity and behavior.

Predictably transforming connectivity in the *Drosophila* brain

Spatial patterning:

Each neuron that comprises the brain has a unique identity, characterized by various morphological and physiological features (Zeng and Sanes 2017). This profile is not determined randomly, but through systematic and tightly regulated neurogenesis across both space and time, even in the mammalian cortex (Mayer et al. 2018). The genetic mechanisms that regulate neurogenesis

thereby shape adult function. Identifying these genetic mechanisms, and their subsequent molecular pathways, could lead to critical connections between developmental history and adult circuitry and broaden our understanding of animal behavior.

Neurons are generated in regular order from neural stem cells (Doe, 2017). While this phenomenon is conserved across species, for the last several decades, *Drosophila* has emerged as a powerful system in which to discover the mechanisms that generate neurons in a stereotyped order. These mechanisms include *spatial, temporal,* and *hemi-lineage identity* (Notch signaling). As neural stem cells, called neuroblasts in *Drosophila*, delaminate from the neuroepithelium they express an array of genes (called spatial transcription factors) across the dorsal-ventral and anterior-posterior axis. Each neuroblast has a unique molecular identity based on where it delaminates in the neuroepithelium. These spatial transcription factors can then instruct the neurons generated by each lineage to innervate their axons or dendrites in discrete neuropil regions within the central nervous system (CNS). Manipulating a single spatial transcription factor through MARCM mutant clonal analysis demonstrated that where an entire lineage innervates its axons and dendrites could be transformed, at least in the larval central brain of *Drosophila* (Sen et al., 2014). In sum, by manipulating spatial factors during neurogenesis, we can now predictably rewire the brain across development. These spatial transcription factors are the first molecular mechanism required to generate neurons with projections to discrete regions of the *Drosophila* CNS neuropil, and thus represent potentially powerful genetic

targets to guide brain development with exquisite control. Yet, they cannot account for how neurons wire into specific neuropil structures, such as glomeruli or layers, to reach their final synaptic target.

Temporal patterning:

After neuroblasts acquire a unique spatial identity, they next express a sequence of transcription factors over time, such that neurons have a unique temporal identity based on birth-order. This phenomenon is conserved across species, and particularly found in several types of *Drosophila* neuroblasts. These include ventral nerve-cord, antennal lobe, mushroom body, optic lobe, and the midline associate type II neuroblasts (Doe, 2017). Each individual neuroblast then expresses a unique sequence of temporal transcription factors, which helps generate neural diversity across the entire CNS. The way in which unique temporal identity genes contribute to axonal and dendritic targeting in the CNS remains poorly understood.

A pioneering study from Tzumin Lee's group in 2012 discovered that manipulating the temporal transcription factor *Chinmo* in distinct neural lineages could rewire glomerulus targeting in the Drosophila antennal lobe. When *Chinmo* is mutated with MARCM clonal analysis, early-born neurons now target a late-born glomerulus (Kao et al., 2012). Before this dissertation, it was entirely unknown whether other temporal identity genes could function in this manner, particularly in the midline type II neuroblast lineages that generate central complex columnar neurons. These lineages are analogous to mammalian

progenitors in the outer subventricular zone of the developing cerebral cortex, which also produce intermediate neural progenitors (INPs) (Hansen et al. 2010). By investigating the molecular mechanisms that generate neural diversity and neural circuits from type II neuroblast lineages, we are beginning to discover the conserved pathways required for mammalian brain development.

In this dissertation, I demonstrate that connectivity can be predictably transformed when we manipulate temporal identity genes in type II neuroblast lineages, particularly INPs. The temporal transcription factor *Eyeless* is not only required to generate EP-G neurons from old INPs; it can also be targeted with RNAi to transform the connectivity of neurons uniquely generated by young INPs. First, I was able to demonstrate that *Eyeless* represses the generation of young INP neurons, such as P-ENs and P-FNs. When *Eyeless* is eliminated from type II neuroblast lineages, P-EN and P-FN neurons are generated by old INPs, creating ectopic copies of these neurons, irrespective of birth-order. I then determined that these 'ectopic P-EN' and 'ectopic P-FN' neurons have precisely the same morphology as endogenous P-EN and P-FN neurons, indicating that they had been transformed according to both molecular markers and morphology. Finally, these 'ectopic P-EN' neurons extend their axons and dendrites into matching glomeruli between neuropils in the central complex, indicating that their anatomical connectivity had also been transformed with *Eyeless* RNAi.

The mammalian homologue for *Eyeless* is the transcription factor PAX6. PAX6 is expressed in cortical progenitors and is required for proper development

across various regions of the mammalian brain (Manuel et al. 2015). PAX6 Target genes have been broadly implicated in autism-spectrum disorders (ASD), and animal behavior (Kikkawa et al. 2019). Thus, studying how Eyeless regulates neuronal fate in the CX, as well as the assembly of neuronal circuits for animal behavior, we can begin to characterize critical components of this pathway, and potentially provide novel avenues for future therapeutics.

Future Directions

There remain dozens more neurons in the adult CX of *Drosophila* that are likely generated by type II NB lineages, yet they are not described in this dissertation. Using the tools described above, each neuron of the CX can have its developmental origin rapidly traced. It could be the case that all CX neurons are generated in discrete temporal windows within type II NB lineages, or that each neuronal cell-type is generated more broadly across larval life. Without first tracing each CX neuron to its origin and birth-date, this remains unknown. From this body of work, I predict that neurons with similar axon/dendrite targeting will have closely similar developmental origins within type II NB lineages.

I demonstrated that the TTF *eyeless* is required to generate matching numbers of E-PG and P-EN CX neurons, yet there remain other candidate temporal identity genes, whose role in generating distinct populations of CX neurons remains unexplored. To date, the temporal identity RNA-binding protein *imp* remains an ideal future candidate, because each of the four CX neurons birth-dated in this dissertation are generated by *imp* positive type II NBs. Future

work could begin to explore if this gene, and others, are required for creating proper numbers of each CX neuron.

I determined that *eyeless* is required to establish proper anatomical connectivity in the central complex but did not demonstrate if neurons can be functionally rewired when *eyeless* is manipulated via RNAi. In future experiments, we could demonstrate that 'ectopic' copies of P-EN neurons, generated when eyeless is manipulated via RNAi, are functionally integrated in the CX circuitry with proper synaptic partners through two-photon calcium imaging of ectopic P-EN neurons. These experiments could help us begin to understand whether ectopic P-EN neurons have the same calcium activity response properties as endogenous P-EN neurons, as animals navigate in the environment.

Finally, I demonstrated that the Eyeless target gene, the transcription factor (TF) Twin of Eyeless (Toy), is required for E-PG axonal targeting to the gall neuropil in the adult brain, yet it is impossible to determine why this phenotype occurred without first characterizing Toy target genes in E-PG neurons. It could be that Toy is regulating axonal growth or axon guidance, but without demonstrating the exact pathway from this TF to its downstream effectors, such as cell-surface molecules, these remain as two distinct hypotheses. Several approaches could determine which gene, or array of genes, Toy is regulating at the gall in E-PG neurons. A candidate knockdown RNAi screen of cell-surface molecules could uncover phenotypes similar to those described in this dissertation, when Toy was knocked down with RNAi in E-PG neurons.

Uncovering the mechanism downstream of Toy that regulates axonal connectivity at the gall in E-PG neurons could provide the first link between a temporal identity gene and cell-surface molecule expression. This remains a compelling concept that is entirely unexplored in the field to date.

APPENDIX A: RESOURCES AND METHODS

Table 1: Key Resources

Reagent type	Designation	Source	ID	Extra info
Species (*Drosophila melanogaster*)	UAS-FLP	BDSC	#4539	FLP enzyme under UAS control
Species (*Drosophila melanogaster*)	R9D11-Gal4	BDSC	#40731	Young INP Gal4 driver
Species (*Drosophila melanogaster*)	R37G12-lexA	BDSC	#52765	PF-R lexA driver
Species (*Drosophila melanogaster*)	R60D05-lexA	BDSC	#52867	E-PG lexA driver
Species (*Drosophila melanogaster*)	R12D09-lexA	BDSC	#54419	P-EN lexA driver
Species (*Drosophila melanoga*	R16D01-lexA	BDSC	#52503	P-FN lexA driver

ster)				
Species (*Drosophila melanogaster*)	lexAop(FRT.stop)mCD8::GFP	BDSC	#57588	FLP-out membrane bound GFP under lexAop control
Species (*Drosophila melanogaster*)	ts.Tubulin-Gal80 (20)	BDSC	#7019	temperature sensitive Gal80
Species (*Drosophila melanogaster*)	20xUAS-FLP.PEST	BDSC	#55807	FLP enzyme under 20xUAS control
Species (*Drosophila melanogaster*)	OK107-Gal4	BDSC	#854	Eyeless enhancer trap Gal4 for old INPs
Species (*Drosophila melanogaster*)	UAS-mCherryRNAi	BDSC	#35787	Control RNAi under UAS control
Species (*Drosophila melanogaster*)	UAS-EyelessRNAi	BDSC	#32486	Eyeless RNAi under UAS control
Species	13xlexAop-myr::GFP	BDSC	#3221	membran

(*Drosophila melanogaster*)			0	e bound GFP under 13xlexAop control
Species (*Drosophila melanogaster*)	R16B06-Gal4	BDSC	#45811	old INP Gal4 driver
Species (*Drosophila melanogaster*)	UAS-FLP, Act5c(FRT.CD2)Gal4 ; ; R12E09-Gal4, UAS-mCD8::GFP	This work		INP immortalization driver expressing membrane bound GFP
Species (*Drosophila melanogaster*)	lexAop(FRT.stop)HA::CD4.T2A.Brp.mCherry	BDSC	#56518	FLP-out fluorensent labeling of Brp
Species (*Drosophila melanogaster*)	ss00096-Gal4	Rubin Lab (Janelia)		E-PG split Gal4 driver
Species (*Drosophila melanogaster*)	Empty-vector split Gal4	Rubin Lab (Janelia)		Control split Gal4 driver

Species (*Drosophila melanogaster*)	UAS-ToyRNAi	BDSC	#33679	Toy RNAi under UAS control
Species (*Drosophila melanogaster*)	lexAop.tdTomato.myr, brp(FRT.stop)V5-2A-lexA-VP16	BDSC	#56142	STaR FLP-out labeling of synaptic terminals
Species (*Drosophila melanogaster*)	10xUAS-myr::HA	BDSC	#62145	membrane bound HA under UAS control
Species (*Drosophila melanogaster*)	R19G02-Gal4	BDSC	#48860	developmental E-PG Gal4
Species (*Drosophila melanogaster*)	UAS-Kir2.1	Giraldo et al., (2018)		Inward rectifying K+ channel under UAS control
Antibody, polyclonal	Chicken anti-GFP	Abcam (Eugene, OR)		1:1000
Antibody, polyclonal	Rabbit anti-Toy	Desplan lab		1:1000

		(NYU)		
Antibody, polyclonal	Guinea-pig anti-Runt	Desplan lab (NYU)		1:1000
Antibody, monoclonal	Mouse anti-nc82	DSHB (Iowa City, IA)		1:50
Antibody, polyclonal	Rabbit anti-V5	Cell Signaling (Danvers MA)		1:400
Antibody, polyclonal	Rabbit Anti HA	Columbia Biosciences (Frederick MD)		1:400
Antibody, polyclonal	Secondary antibodies	Thermofisher (Eugene, OR)		1:400

Table 2: Genotypes

Fly genotypes used in each experiment	**Synopsis**
UAS-FLP ; R9D11-Gal4 X R37G12-lexA ; lexAop(FRT.stop)mCD8::GFP	PF-R labeling
UAS-FLP ; R9D11-Gal4 X R60D05-lexA ; lexAop(FRT.stop)mCD8::GFP	E-PG labeling
UAS-FLP ; R9D11-Gal4 X R12D09-lexA ; lexAop(FRT.stop)mCD8::GFP	P-EN labeling
UAS-FLP ; R9D11-Gal4 X R16D01-lexA ; lexAop(FRT.stop)mCD8::GFP	P-FN labeling
20XUAS-FLP.PEST ; ts.Tubulin-Gal80 (20) ; R9D11-Gal4 X R37G12-lexA ; lexAop(FRT.stop)mCD8::GFP	PF-R birthdating
20XUAS-FLP.PEST ; ts.Tubulin-Gal80 (20) ; R9D11-Gal4 X R60D05-lexA ; lexAop(FRT.stop)mCD8::GFP	E-PG birthdating

20XUAS-FLP.PEST ; ts.Tubulin-Gal80 (20) ; R9D11-Gal4 X R12D09-lexA ; lexAop(FRT.stop)mCD8::GFP	P-EN birthdating
20XUAS-FLP.PEST ; ts.Tubulin-Gal80 (20) ; R9D11-Gal4 X R16D01-lexA ; lexAop(FRT.stop)mCD8::GFP	P-FN birthdating
UAS-FLP ; R9D11-Gal4 X R37G12-lexA ; lexAop(FRT.stop)mCD8::GFP	PF-R labeling
UAS-FLP ; R9D11-Gal4 X R60D05-lexA ; lexAop(FRT.stop)mCD8::GFP	E-PG labeling
UAS-FLP ; R9D11-Gal4 X R12D09-lexA ; lexAop(FRT.stop)mCD8::GFP	P-EN labeling
UAS-FLP ; R9D11-Gal4 X R16D01-lexA ; lexAop(FRT.stop)mCD8::GFP	P-FN labeling
OK107-Gal4 X 20XUAS-FLP.PEST ; R37G12-lexA ; lexAop(FRT.stop)mCD8::GFP	PF-R labeling old INP
OK107-Gal4 X 20XUAS-FLP.PEST ; R60D05-lexA ; lexAop(FRT.stop)mCD8::GFP	E-PG labeling old INP
OK107-Gal4 X 20XUAS-FLP.PEST ; R12D09-lexA ; lexAop(FRT.stop)mCD8::GFP	P-EN labeling old INP
OK107-Gal4 X 20XUAS-FLP.PEST ; R16D01-lexA ; lexAop(FRT.stop)mCD8::GFP	P-FN labeling old INP
13xlexAop-myr::GFP ; UAS-mCherryRNAi X R37G12-lexA ; R16B06-Gal4	PF-R labeling WT
13xlexAop-myr::GFP ; UAS-mCherryRNAi X R60D05-lexA ; R16B06-Gal4	E-PG labeling WT
UAS-FLP, Act5c(FRT.CD2)Gal4 ; ; R12E09-Gal4, UAS-mCD8::GFP X UAS-mCherryRNAi	INP lineage tracing WT
13xlexAop-myr::GFP ; UAS-EyelessRNAi X R37G12-lexA ; R16B06-Gal4	PF-R labeling Ey-RNAi
13xlexAop-myr::GFP ; UAS-EyelessRNAi X R60D05-lexA ; R16B06-Gal4	E-PG labeling Ey-RNAi
UAS-FLP, Act5c(FRT.CD2)Gal4 ; ; R12E09-Gal4, UAS-mCD8::GFP X UAS-EyelessRNAi	INP lineage tracing Ey-RNAi
13xlexAop-myr::GFP ; UAS-mCherryRNAi X R12D09-lexA ; R16B06-Gal4	P-EN labeling WT
13xlexAop-myr::GFP ; UAS-mCherryRNAi X R16D01-lexA ; R16B06-Gal4	P-FN labeling WT

UAS-FLP, Act5c(FRT.CD2)Gal4 ; ; R12E09-Gal4, UAS-mCD8::GFP X UAS-mCherryRNAi	INP lineage tracing WT
13xlexAop-myr::GFP ; UAS-EyelessRNAi X R12D09-lexA ; R16B06-Gal4	P-EN labeling Ey-RNAi
13xlexAop-myr::GFP ; UAS-EyelessRNAi X R16D01-lexA ; R16B06-Gal4	P-FN labeling Ey-RNAi
UAS-FLP, Act5c(FRT.CD2)Gal4 ; ; R12E09-Gal4, UAS-mCD8::GFP X UAS-EyelessRNAi	INP lineage tracing Ey-RNAi
R37G12-lexA X 13xlexAop-myr::GFP	PF-R labeling
R60D05-lexA X 13xlexAop-myr::GFP	E-PG labeling
R12D09-lexA X 13xlexAop-myr::GFP	P-EN labeling
R16D01-lexA X 13xlexAop-myr::GFP	P-FN labeling
R12D09-lexA ; lexAop(FRT.stop)mCD8::GFP ; OK107-Gal4 X 20XUAS-FLP.PEST ; ts.Tubulin-Gal80 (20) ; UAS-mCherryRNAi	Ectopic P-EN WT
R12D09-lexA ; lexAop(FRT.stop)mCD8::GFP ; OK107-Gal4 X 20XUAS-FLP.PEST ; ts.Tubulin-Gal80 (20) ; UAS-EyelessRNAi	Ectopic P-EN Ey-RNAi
R12D09-lexA ; lexAop(FRT.stop)HA::CD4.T2A.Brp.mCherry ; OK107-Gal4 X 20XUAS-FLP.PEST ; ts.Tubulin-Gal80 (20) ; UAS-EyelessRNAi	Ectopic P-EN brp Ey-RNAi
R16D01-lexA ; R16B06-Gal4 x 13xlexAop-myr::GFP ; UAS-mCherryRNAi	WT P-FN neuron morph.
R16D01-lexA ; R16B06-Gal4 x 13xlexAop-myr::GFP ; UAS-EyelessRNAi	Ey-RNAi P-FN neuron morph.
R16B06-Gal4 X ts.Tubulin-Gal80 (10) ; UAS-EyelessRNAi	no heat pulse control nc82
R16B06-Gal4 X ts.Tubulin-Gal80 (10) ; UAS-EyelessRNAi	heat pulse nc82
R16B06-Gal4 X ts.Tubulin-Gal80 (10) ; UAS-EyelessRNAi	no heat pulse control behavior
R16B06-Gal4 X ts.Tubulin-Gal80 (10) ; UAS-mCherryRNAi	heashock control behavior

R16B06-Gal4 X ts.Tubulin-Gal80 (10) ; UAS-EyelessRNAi	heat pulse exp. behavior
10xUAS-myr::GFP ; R19G02-Gal4 X UAS-mCherryRNAi	E-PG dev. driver control
10xUAS-myr::GFP ; R19G02-Gal4 X UAS-ToyRNAi	E-PG dev. driver Toy-LOF
10xUAS-myr::HA ; ss00096-Gal4 X UAS-mCherryRNAi	E-PG split driver control
10xUAS-myr::HA ; ss00096-Gal4 X UAS-ToyRNAi	E-PG split driver Toy-LOF
20XUAS-FLP.PEST ; ss00096-Gal4 X lexAop-tdTomato.myr, brp(FRT.stop)V5-2A-lexA-VP16 ; UAS-mCherryRNAi	E-PG STaR control
20XUAS-FLP.PEST ; ss00096-Gal4 X lexAop-tdTomato.myr, brp(FRT.stop)V5-2A-lexA-VP16 ; UAS-ToyRNAi	E-PG STaR Toy-LOF
R16B06-Gal4 X ts.Tubulin-Gal80 (10) ; UAS-EyelessRNAi	no heat pulse control behavior
R16B06-Gal4 X ts.Tubulin-Gal80 (10) ; UAS-mCherryRNAi	heashock control behavior
R16B06-Gal4 X ts.Tubulin-Gal80 (10) ; UAS-EyelessRNAi	heat pulse exp. behavior
Empty Split-Gal4 x UAS-Kir2.1	E-PG control behavior
ss00096 Split-Gal4 x UAS-Kir2.1	E-PG silenced behavior
Empty Split-Gal4 x UAS-Kir2.1	E-PG control behavior
ss00096 Split-Gal4 x UAS-Kir2.1	E-PG silenced behavior
Empty Split-Gal4 x UAS Toy-RNAi	Toy-RNAi control behavior
ss00096 Split-Gal4 x UAS Toy-RNAi	Toy-RNAi exper. behavior

Methods

Standardizing larval development at different temperatures

All larvae were grown at 25°C unless noted, and all hours after larval hatching are standardized to grow wild type at 25°C based on published conversions: 18°C is 2.25x slower than 25°C, and 29°C is 1.03x faster than 25°C (Powsner 1935).

Immunohistochemistry

Primary and secondary antibodies, see Key Resources Table, above. Adult brain dissections were conducted at room temperature with 2-5 day old adult females. Adult brains were dissected in 2% formaldehyde solution in Phosphate-Buffered Saline with .5% Triton-X (PBST) and incubated for 55 minutes before applying an overnight block solution (5% Goat/Donkey serum, Vector Laboratories) at 4^{o}C. Brains were then washed in PBST for one hour before applying an overnight primary mix at 4^{o}C. Then, brains were washed for one hour at room temperature in PBST, before applying an overnight secondary mix at 4^{o}C. Finally, brains were mounted in 90% glycerol, and imaged immediately.

Imaging, data acquisition, and image analysis

Fluorescent images were acquired on a Zeiss LSM 700. Adult brain cell counting was performed using the Fiji cell counter plug in, and statistical analysis (Student's T test) was done in Excel. Figures were assembled in Illustrator (Adobe). Relative Brp-density was quantified in Fiji; maximum intensity projections were made, a rectangular ROI selected around the Gall, and a histogram plot of pixel intensity was generated. Background for image was calculated in neighboring ROIs and

subtracted from each individual histogram plot-value. Intensity values were then summed together to calculate total intensity, and this was divided by Gall total area, calculated manually in Fiji using polygon selection tool. Qualitative measurements of Gall defects were made by observing whether the total area of the Gall had been reduced, or entirely eliminated, through visual observations in FIJI.

Fly tethering for flight behavior

We used 3-4 day old females for behavioral experiments. We tethered flies under cold anesthesia, gluing a tungsten wire to the anterior notum with UV-cured glue (Bondic). The head was immobilized relative to the body with a small amount of glue between the head and thorax. Flies recovered for at least 20 min prior to behavioral testing.

Flight Arena and behavioral protocol

We coupled the angular velocity of a visual stimulus that was presented via LED panels to the continuously measured difference in wing stroke amplitude. Stroke amplitude was tracked at 60 Hz via Kinefly, a previously described video tracking system (Suver et al, 2016). A digital camera equipped with macro lens (Computar MLM3x-MP) and IR filter (Hoya) captured wing images from a 45° mirror positioned beneath the fly. Backlit illumination of wings was provided by a collimated infrared LED above fly (Thorlabs #M850L3). We displayed visual stimuli using a circular arena of 2 rows of 12 LED panels (24 panels total). Each panel had 64 pixels (Betlux #BL-M12A881PG-11, λ=525 nm) and was controlled

using hardware and firmware (IORodeo.com) as previously described (Giraldo et al. 2018).The gain between stimulus angular velocity and wing stroke amplitude difference was 4.75°/s per degree of wing stroke difference. The sun stimulus was a single LED pixel which is ~2.4° on fly retina (Giraldo et al. 2018) ~30deg above fly. The stripe was 4 pixels wide and 16 pixels high (15° by 60°). Flight experiments were controlled by custom scripts (Warren 2019) in the ROS environment. Incoming video was collected at 60 Hz and stimulus position data (i.e. the flight heading) at 200 Hz. In each experiment, flies navigated in closed loop to the sun stimulus in two distinct 5 min trials, which were separated by a 5 min rest period, during which we gave flies a small piece of paper to manipulate with their legs. Following the second sun flight, flies flew for 5 min in closed loop to the stripe stimulus. We discarded flights in which a fly stopped flying more than once during a sun or stripe presentation; furthermore, we discarded flights from flies that did not complete the two 5 min sun flights.

Behavioral Data Analysis

All data analysis was conducted using custom scripts in Python. The circular mean heading of a flight was computed as the angle of resultant vector obtained via vector summation, treating each angular heading measurement as a unit vector. To determine the vector strength, we normalized the length of the resultant vector by the number of individual headings.

Statistics

Data represent mean +/- standard deviation. Two-tailed Student's t-tests were used to assess statistical significance of anatomical data, with *P<0.05; **P<0.01; ***P<0.001. To determine the significance of differences in the mean of the vector strength and heading distribution between groups, we used Fisher's exact test with 10,000 permutations (Fisher, 1937). To avoid pseudoreplication, we permuted across flies rather than flights. We computed a 95% confidence interval of the circular mean of each heading distribution by bootstrapping from the observed data. For each experimental condition, we resampled with replacement from the observed flight data (resampling across flies not flights) to create 10,000 distributions of matched size to the observed data set. Confidence intervals were computed from the circular means of these 10,000 distributions. For analysis of the heading distributions and confidence intervals, we considered flights with a vector strength above a minimum threshold of 0.2.

APPENDIX B: GENETIC SCHEMATIC FOR EACH EXPERIMENT

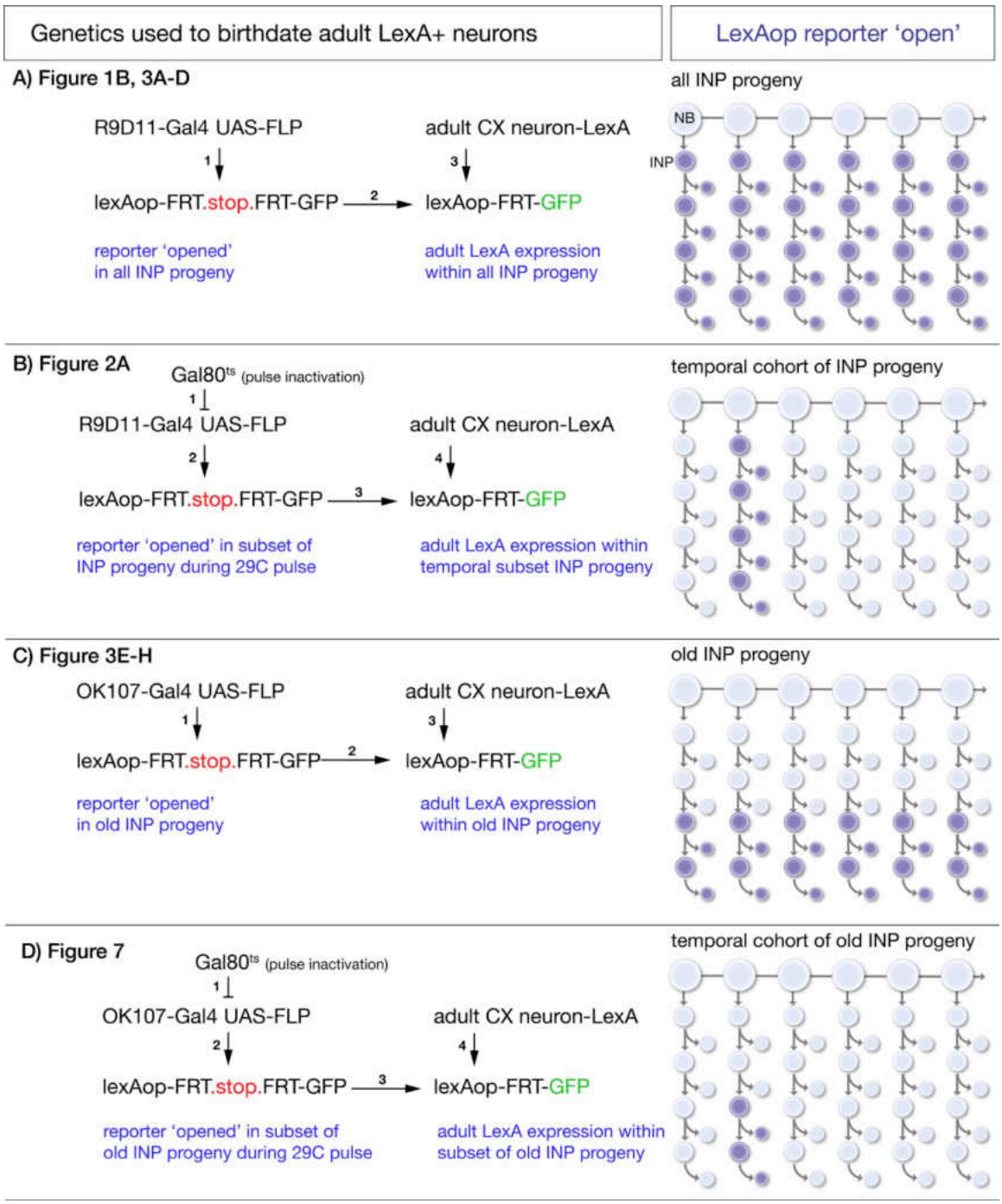

(A) Identifying columnar neuron subtypes derived from all INPs. *R9D11-Gal4* drives expression of FLP which excises an *FRT-stop* in all INPs and their

progeny. This allows columnar neuron specific LexA lines to drive GFP expression if the neurons derive from INPs.

(B) Identifying the time during the neuroblast lineage that produces each columnar neuron subtype. A pulse of 29^{o}C disables ts.Gal80 to allow *R9D11-Gal4* to excise *FRT.stop* in the INPs present during the heat pulse. This allows columnar neuron specific LexA lines to drive GFP expression if the neurons derive from INPs born from the type II neuroblast at the time of heat pulse.

(C) Identifying columnar neuron subtypes derived from young or old INPs. *OK107-Gal4* drives expression of FLP which excises an *FRT-stop* only in old INPs and their progeny. This allows columnar neuron specific LexA lines to drive GFP expression if the neurons derive from old INPs. Lack of expression shows the neurons are derived from young INPs.

(D) Identifying the time during the neuroblast lineage that produces each old INP-derived columnar neuron subtype. A pulse of 29^{o}C disables ts.Gal80 to allow *OK107-Gal4* to excise the *FRT.stop* in the INPs present during the heat pulse. This allows columnar neuron specific LexA lines to drive GFP expression if the neurons derive from INPs present at the time of heat pulse.

REFERENCES CITED

Andrade, I. V, Riebli, N., Nguyen, B. M., Omoto, J. J., Andrade, I. V, Riebli, N., … Hartenstein, V. (2019). Developmentally Arrested Precursors of Pontine Neurons Establish an Embryonic Blueprint of the Drosophila Central Complex. *Current Biology*, *29*(3), 412–425.e3. https://doi.org/10.1016/j.cub.2018.12.012

Bello, B. C., Izergina, N., Caussinus, E., & Reichert, H. (2008). Amplification of neural stem cell proliferation by intermediate progenitor cells in Drosophila brain development. *Neural Development*, *3*(1). https://doi.org/10.1186/1749-8104-3-5

Benson, D. L., Colman, D. R., & Huntley, G. W. (2001). Molecules, maps and synapse specificity. *Nature Reviews Neuroscience*, *2*(12), 899–909. https://doi.org/10.1038/35104078

Betley, J. N., Wright, C. V. E., Kawaguchi, Y., Erdélyi, F., Szabó, G., Jessell, T. M., & Kaltschmidt, J. A. (2009). Stringent Specificity in the Construction of a GABAergic Presynaptic Inhibitory Circuit. *Cell*, *139*(1), 161–174. https://doi.org/10.1016/j.cell.2009.08.027

Boone, J. Q., & Doe, C. Q. (2008). Identification of Drosophila type II neuroblast lineages containing transit amplifying ganglion mother cells. *Developmental Neurobiology*, *68*(9), 1185–1195. https://doi.org/10.1002/dneu.20648

Couto, A., Alenius, M., & Dickson, B. J. (2005). Molecular, anatomical, and functional organization of the Drosophila olfactory system. *Current Biology*, *15*(17), 1535–1547. https://doi.org/10.1016/j.cub.2005.07.034

Dickson, B. J. (2008). Molecular Mechanisms of Axon Guidance. *Science*, *1959*(2002). https://doi.org/10.1126/science.1072165

Doe, C. Q. (2017). Temporal Patterning in the Drosophila CNS. *Annual Review of Cell and Developmental Biology Annu. Rev. Cell Dev. Biol*, *33*, 219–240. https://doi.org/10.1146/annurev-cellbio-111315

Donlea, J. M., Pimentel, D., Talbot, C. B., Kempf, A., Omoto, J. J., Hartenstein, V., & Miesenböck, G. (2018). Recurrent Circuitry for Balancing Sleep Need and Sleep. *Neuron*, *97*(2), 378–389.e4. https://doi.org/10.1016/j.neuron.2017.12.016

Dubowy, C., & Sehgal, A. (2017). Circadian rhythms and sleep in Drosophila melanogaster. *Genetics*, *205*(4), 1373–1397. https://doi.org/10.1534/genetics.115.185157

Enriquez, J., Venkatasubramanian, L., Baek, M., Peterson, M., Aghayeva, U., & Mann, R. S. (2015). Specification of Individual Adult Motor Neuron Morphologies by Combinatorial Transcription Factor Codes. *Neuron*, *86*(4), 955–970. https://doi.org/10.1016/j.neuron.2015.04.011

Farnsworth, D. R., Bayraktar, O. A., Doe, C. Q., Farnsworth, D. R., Bayraktar, O. A., & Doe, C. Q. (2015). Aging Neural Progenitors Lose Competence to Respond to Mitogenic Notch Signaling Article Aging Neural Progenitors Lose Competence to Respond to Mitogenic Notch Signaling. *CURBIO*, *25*(23), 3058–3068. https://doi.org/10.1016/j.cub.2015.10.027

Fishilevich, E., & Vosshall, L. B. (2005). Genetic and functional subdivision of the Drosophila antennal lobe. *Current Biology*, *15*(17), 1548–1553. https://doi.org/10.1016/j.cub.2005.07.066

Franconville, R., Beron, C., & Jayaraman, V. (2018). Building a functional connectome of the drosophila central complex. *ELife*, *7*, 1–24. https://doi.org/10.7554/eLife.37017

Giraldo, Y. M., Leitch, K. J., Ros, I. G., Warren, T. L., Weir, P. T., Dickinson, M. H., … Weir, P. T. (2018). Sun Navigation Requires Compass Neurons in Sun Navigation Requires Compass Neurons in Drosophila. *Current Biology*, *28*(17), 2845–2852.e4. https://doi.org/10.1016/j.cub.2018.07.002

Gold, J. I., & Shadlen, M. N. (2001). Neural computations that underlie decisions about sensory stimuli. *Trends in Cognitive Sciences*, *5*(1), 10–16. https://doi.org/10.1016/S1364-6613(00)01567-9

Green, J., Adachi, A., Shah, K. K., Hirokawa, J. D., Magani, P. S., & Maimon, G. (2017). A neural circuit architecture for angular integration in Drosophila. *Nature Publishing Group*, *546*(7656), 101–106. https://doi.org/10.1038/nature22343

Green, J., Vijayan, V., Pires, P. M., Adachi, A., & Maimon, G. (2018). Walking Drosophila aim to maintain a neural heading estimate at an internal goal angle. *BioRxiv*, 315796. https://doi.org/10.1101/315796

Hainsworth, F. R., Collins, B. G., & Wolf, L. L. (1977). Division of Comparative Physiology and Biochemistry , Society for Integrative and Comparative Biology The Function of Torpor in Hummingbirds Published by : University of Chicago Press . Sponsored by the Division of Comparative Physiology and Biochemistry, *3*(3), 215–222.

Harris, R. M., Pfeiffer, B. D., Rubin, G. M., & Truman, J. W. (2015). Neuron hemilineages provide the functional ground plan for the Drosophila ventral nervous system. *ELife*, *4*(JULY2015), 1–34. https://doi.org/10.7554/eLife.04493

He, M., & Hutchinson, J. W. (1991). Kinking of a crack out of an interface: tabulated solution coefficients. *Harvard University Report MECH-113A*, *74*(197664), 767–771. https://doi.org/10.1038/681

Heinze, S. (2017). ScienceDirect Unraveling the neural basis of insect navigation. *Current Opinion in Insect Science*, *24*(Figure 1), 58–67. https://doi.org/10.1016/j.cois.2017.09.001

Hoch, R. G., Duponchel, J. P., Cocking, B. J., & Bryce, W. D. (1973). Studies of the influence of density on jet noise. *Journal of Sound and Vibration*, *28*(4), 649–668. https://doi.org/10.1016/S0022-460X(73)80141-5

Homem, C. C. F., Reichardt, I., Berger, C., Lendl, T., & Knoblich, J. A. (2013). Long-term live cell imaging and automated 4D analysis of Drosophila neuroblast lineages. *PLoS ONE*, *8*(11), 1–10. https://doi.org/10.1371/journal.pone.0079588

Homem, C. C. F., Saini, N., Burkard, T. R., Jiang, Y., Reichert, H., Eroglu, E., & Knoblich, J. A. (2014). SWI/SNF Complex Prevents Lineage Reversion and Induces Temporal Patterning in Neural Stem Cells. *Cell*, *156*(6), 1259–1273. https://doi.org/10.1016/j.cell.2014.01.053

Isshiki, T., Pearson, B., Holbrook, S., & Doe, C. Q. (2001). Drosophila neuroblasts sequentially express transcription factors which specify the temporal identity of their neuronal progeny. *Cell*, *106*(4), 511–521. https://doi.org/10.1016/S0092-8674(01)00465-2

Ito, M., Masuda, N., Shinomiya, K., Endo, K., & Ito, K. (2013). Systematic analysis of neural projections reveals clonal composition of the Drosophila brain. *Current Biology*, *23*(8), 644–655. https://doi.org/10.1016/j.cub.2013.03.015

Jefferis, G. S. X. E., Marin, E. C., Stocker, R. F., & Luo, L. (2001). Target neuron prespecification in the olfactory map of Drosophila. *Nature*, *414*(6860), 204–208. https://doi.org/10.1038/35102574

Joo, W. J., Sweeney, L. B., Liang, L., & Luo, L. (2013). Linking cell fate, trajectory choice, and target selection: Genetic analysis of sema-2b in olfactory axon targeting. *Neuron*, *78*(4), 673–686. https://doi.org/10.1016/j.neuron.2013.03.022

Kao, C. F., Yu, H. H., He, Y., Kao, J. C., & Lee, T. (2012). Hierarchical Deployment of Factors Regulating Temporal Fate in a Diverse Neuronal Lineage of the Drosophila Central Brain. *Neuron*, *73*(4), 677–684. https://doi.org/10.1016/j.neuron.2011.12.018

Karamipour, N., Fathipour, Y., Talebi, A. A., Asgari, S., & Mehrabadi, M. (2018). Small interfering RNA pathway contributes to antiviral immunity in Spodoptera frugiperda (Sf9) cells following Autographa californica multiple nucleopolyhedrovirus infection. *Insect Biochemistry and Molecular Biology*, *101*, 24–31. https://doi.org/10.1016/j.ibmb.2018.07.004

Kim, S., Rouault, H., Seelig, J. D., Druckmann, S., & Jayaraman, V. (2016). Ring attractor dynamics in the Drosophila central complex. *Society for Neuroscience*, *853*(San Diego, CA), 849–853. https://doi.org/10.1126/science.aal4835

Lacin, H., Zhu, Y., Wilson, B. A., & Skeath, J. B. (2014). Transcription factor expression uniquely identifies most postembryonic neuronal lineages in the Drosophila thoracic central nervous system. *Development*, *141*(5), 1011–1021. https://doi.org/10.1242/dev.102178

Leone, D. P., Srinivasan, K., Chen, B., Alcamo, E., & McConnell, S. K. (2008). The determination of projection neuron identity in the developing cerebral cortex. *Current Opinion in Neurobiology*, *18*(1), 28–35. https://doi.org/10.1016/j.conb.2008.05.006

Li, H., Shuster, S. A., Li, J., & Luo, L. (2018). Linking neuronal lineage and wiring specificity. *Neural Development*, *13*(1), 1–19. https://doi.org/10.1186/s13064-018-0102-0

Li, Y., Lu, H., Cheng, P. L., Ge, S., Xu, H., Shi, S. H., & Dan, Y. (2012). Clonally related visual cortical neurons show similar stimulus feature selectivity. *Nature*, *486*(7401), 118–121. https://doi.org/10.1038/nature11110

Lichtneckert, R., & Reichert, H. (2005). Insights into the urbilaterian brain: Conserved genetic patterning mechanisms in insect and vertebrate brain development. *Heredity*, *94*(5), 465–477. https://doi.org/10.1038/sj.hdy.6800664

Lin, C., Chuang, C., Hua, T., Chen, C., Dickson, B. J., & Greenspan, R. J. (2013). A Comprehensive Wiring Diagram of the Protocerebral Bridge for Visual Information Processing in the Drosophila Brain. *CellReports*, *3*(5), 1739–1753. https://doi.org/10.1016/j.celrep.2013.04.022

Liu, Z., Nern, A., & Cell-intrinsic, S. (2017). Stem Cell-Intrinsic, Seven-up-Triggered Temporal Factor Gradients Diversify Intermediate Neural Progenitors. *Current Biology*, *27*(9), 1303–1313. https://doi.org/10.1016/j.cub.2017.03.047

Lovick, J. K., Omoto, J. J., Ngo, K. T., & Hartenstein, V. (2017). Development of the anterior visual input pathway to the Drosophila central complex. *Journal of Comparative Neurology*, *525*(16), 3458–3475. https://doi.org/10.1002/cne.24277

Lovick, J. K., Ngo, K. T., Omoto, J. J., Wong, D. C., Nguyen, J. D., & Hartenstein, V. (2013). Postembryonic lineages of the Drosophila brain: I. Development of the lineage-associated fiber tracts. *Developmental Biology*, *384*(2), 228–257. https://doi.org/10.1016/j.ydbio.2013.07.008

Marin, E. C., Altman, J., Truman, J. W., Williams, D. W., & Moats, W. (2009). Role of Notch signaling in establishing the hemilineages of secondary neurons in Drosophila melanogaster. *Development*, *137*(1), 53–61. https://doi.org/10.1242/dev.041749

Melnattur, K. V., & Lee, C. H. (2011). Visual circuit assembly in Drosophila. *Developmental Neurobiology*, *71*(12), 1286–1296. https://doi.org/10.1002/dneu.20894

Mitchell, S. P., Brown, M. P., Kolodkin, A. L., Wu, M. N., Tabuchi, M., & Xie, X. (2017). The laminar organization of the Drosophila ellipsoid body is semaphorin-dependent and prevents the formation of ectopic synaptic connections. *ELife*, *6*(Cx), 1–33. https://doi.org/10.7554/elife.25328

Molyneaux, B. J., Arlotta, P., Menezes, J. R. L., & Macklis, J. D. (2007). Neuronal subtype specification in the cerebral cortex. *Nature Reviews Neuroscience*, *8*(6), 427–437. https://doi.org/10.1038/nrn2151

Ohtsuki, G., Nishiyama, M., Yoshida, T., Murakami, T., Histed, M., Lois, C., & Ohki, K. (2012). Similarity of visual selectivity among clonally related neurons in visual cortex. *Neuron*, *75*(1), 65–72. https://doi.org/10.1016/j.neuron.2012.05.023

Olsen, S. R., & Wilson, R. I. (2008). Cracking neural circuits in a tiny brain: new approaches for understanding the neural circuitry of Drosophila. *Trends in Neurosciences*, *31*(10), 512–520. https://doi.org/10.1016/j.tins.2008.07.006

Pereanu, W. (2006). Neural Lineages of the Drosophila Brain: A Three-Dimensional Digital Atlas of the Pattern of Lineage Location and Projection at the Late Larval Stage. *Journal of Neuroscience*, *26*(20), 5534–5553. https://doi.org/10.1523/JNEUROSCI.4708-05.2006

Pfeiffer, K., & Homberg, U. (2013). Organization and Functional Roles of the Central Complex in the Insect Brain. *Annual Review of Entomology*, *59*(1), 165–184. https://doi.org/10.1146/annurev-ento-011613-162031

Pinto-Teixeira, F., Koo, C., Rossi, A. M., Neriec, N., Bertet, C., Li, X., … Desplan, C. (2018). Development of Concurrent Retinotopic Maps in the Fly Motion Detection Circuit. *Cell*, *173*(2), 485–498.e11. https://doi.org/10.1016/j.cell.2018.02.053

Reichert, H., & Simeone, A. (2001). Developmental genetic evidence for a monophyletic origin of the bilaterian brain. *Philosophical Transactions of the Royal Society B: Biological Sciences*, *356*(1414), 1533–1544. https://doi.org/10.1098/rstb.2001.0972

Reichert, H. (2009). Opinion piece: Evolutionary conservation of mechanisms for neural regionalization, proliferation and interconnection in brain development. *Biology Letters*, *5*(1), 112–116. https://doi.org/10.1098/rsbl.2008.0337

Riebli, N., Viktorin, G., & Reichert, H. (2013). Early-born neurons in type II neuroblast lineages establish a larval primordium and integrate into adult circuitry during central complex development in Drosophila. *Neural Development*, *8*(1), 1–17. https://doi.org/10.1186/1749-8104-8-6

Rolland, V., Kinsey, K. A., Emery, G., Betschinger, J., Bowman, S. K., & Knoblich, J. A. (2008). The Tumor Suppressors Brat and Numb Regulate Transit-Amplifying Neuroblast Lineages in Drosophila. *Developmental Cell*, *14*(4), 535–546. https://doi.org/10.1016/j.devcel.2008.03.004

Rossi, A. M., Fernandes, V. M., & Desplan, C. (2017). ScienceDirect Timing temporal transitions during brain development. *Current Opinion in Neurobiology*, *42*, 84–92. https://doi.org/10.1016/j.conb.2016.11.010

Sen, S., Cao, D., Choudhary, R., Biagini, S., Wang, J. W., Reichert, H., & VijayRaghavan, K. (2014). Genetic transformation of structural and functional circuitry rewires the Drosophila brain. *ELife*, *3*, 1–27. https://doi.org/10.7554/eLife.04407

Shadlen, M. N., Britten, K., Newsome, W., & Movshon, J. (1996). A computational analysis of the relationship between neuronal and behavioral responses to visual motion. *J. Neurosci.*, *16*(4), 1486–1510. Retrieved from http://www.jneurosci.org/content/16/4/1486.short

Skeath, J. B., & Thor, S. (2003). Genetic control of Drosophila nerve cord development. *Current Opinion in Neurobiology*, *13*(1), 8–15. https://doi.org/10.1016/S0959-4388(03)00007-2

Spana, E. P., & Doe, C. Q. (1996). Numb antagonizes Notch signaling to specify sibling neuron cell fates. *Neuron*, *17*(1), 21–26. https://doi.org/10.1016/S0896-6273(00)80277-9

Syed, M. H., Mark, B., & Doe, C. Q. (2017). Steroid hormone induction of temporal gene expression in Drosophila brain neuroblasts generates neuronal and glial diversity. *ELife*, *6*, 1–23. https://doi.org/10.7554/elife.26287

Tada, T., & Sheng, M. (2006). Molecular mechanisms of dendritic spine morphogenesis. *Current Opinion in Neurobiology*, *16*(1), 95–101. https://doi.org/10.1016/j.conb.2005.12.001

Technau, G. M., Berger, C., & Urbach, R. (2006). Generation of cell diversity and segmental pattern in the embryonic central nervous system of Drosophila. *Developmental Dynamics*, *235*(4), 861–869. https://doi.org/10.1002/dvdy.20566

Truman, J. W., Moats, W., Altman, J., Marin, E. C., & Williams, D. W. (2010). Role of Notch signaling in establishing the hemilineages of secondary neurons in Drosophila melanogaster. *Development*, *137*(1), 53–61. https://doi.org/10.1242/dev.041749

Truman, J. W., & Bate, M. (1988). Spatial and temporal patterns of neurogenesis in the central nervous system of Drosophila melanogaster. *Developmental Biology*, *125*(1), 145–157. https://doi.org/10.1016/0012-1606(88)90067-X

Ttha, R. (2008). References and Notes 1. *Science*, *321*(September), 1673–1675. https://doi.org/10.5061/dryad.5t110.Supplementary

Turner-Evans, D., Wegener, S., Rouault, H., Franconville, R., Wolff, T., Seelig, J. D., … Jayaraman, V. (2017). Angular velocity integration in a fly heading circuit. *ELife*, *6*, 1–39. https://doi.org/10.7554/eLife.23496

Ueno, T., Tomita, J., Tanimoto, H., Endo, K., Ito, K., Kume, S., & Kume, K. (2012). Identification of a dopamine pathway that regulates sleep and arousal in Drosophila. *Nature Neuroscience*, *15*(11), 1516–1523. https://doi.org/10.1038/nn.3238

Urbach, R. (2003). Molecular markers for identified neuroblasts in the developing brain of Drosophila. *Development*, *130*(16), 3621–3637. https://doi.org/10.1242/dev.00533

Urbach, R., & Technau, G. M. (2004). Neuroblast formation and patterning during early brain development in Drosophila. *BioEssays*, *26*(7), 739–751. https://doi.org/10.1002/bies.20062

Wilcox, T., & Hirshkowitz, A. (2015). NIH Public Access, *85*(0 1), 1–27. https://doi.org/10.1016/j.neuroimage.2013.08.045.The

Wolff, T., Iyer, N. A., & Rubin, G. M. (2015). Neuroarchitecture and neuroanatomy of the Drosophila central complex: A GAL4-based dissection of protocerebral bridge neurons and circuits. *Journal of Comparative Neurology*, *523*(7), 997–1037. https://doi.org/10.1002/cne.23705

Wolff, T., & Rubin, G. M. (2018). Neuroarchitecture of the Drosophila central complex: A catalog of nodulus and asymmetrical body neurons and a revision of the protocerebral bridge catalog. *Journal of Comparative Neurology*, *526*(16), 2585–2611. https://doi.org/10.1002/cne.24512

Yang, J. S., Odenwald, W. F., Johnston, R., Ren, Q., Wang, Y.-C., Brody, T., … Lee, T. (2013). Drosophila intermediate neural progenitors produce lineage-dependent related series of diverse neurons. *Development*, *141*(2), 253–258. https://doi.org/10.1242/dev.103069

Yang, J. S., Awasaki, T., Yu, H. H., He, Y., Ding, P., Kao, J. C., & Lee, T. (2013). Diverse neuronal lineages make stereotyped contributions to the Drosophila locomotor control center, the central complex. *Journal of Comparative Neurology*. https://doi.org/10.1002/cne.23339

Young, J. M., & Armstrong, J. D. (2010). Structure of the adult central complex in Drosophila: Organization of distinct neuronal subsets. *Journal of Comparative Neurology*, *518*(9), 1500–1524. https://doi.org/10.1002/cne.22284

Yu, H. H., Awasaki, T., Schroeder, M. D., Long, F., Yang, J. S., He, Y., … Lee, T. (2013). Clonal development and organization of the adult Drosophila central brain. *Current Biology*, *23*(8), 633–643. https://doi.org/10.1016/j.cub.2013.02.057

Yu, Y. C., Bultje, R. S., Wang, X., & Shi, S. H. (2009). Specific synapses develop preferentially among sister excitatory neurons in the neocortex. *Nature*, *458*(7237), 501–504. https://doi.org/10.1038/nature07722

Zhu, S., Lin, S., Kao, C. F., Awasaki, T., Chiang, A. S., & Lee, T. (2006). Gradients of the Drosophila Chinmo BTB-Zinc Finger Protein Govern Neuronal Temporal Identity. *Cell*, *127*(2), 409–422. https://doi.org/10.1016/j.cell.2006.08.045

Zhuang, J., Ng, L., Williams, D., Valley, M., Li, Y., Garrett, M., & Waters, J. (2017). An extended retinotopic map of mouse cortex. *ELife*, *6*, 1–29. https://doi.org/10.7554/eLife.18372